ANNUAL REVIEWS

Annual Review of Earth and Planetary Sciences

Flood Basalts and Mass Extinctions

Matthew E. Clapham[1] and Paul R. Renne[2,3]

[1]Department of Earth and Planetary Sciences, University of California, Santa Cruz, California 95064, USA; email: mclapham@ucsc.edu

[2]Berkeley Geochronology Center, Berkeley, California 94709, USA; email: prenne@bgc.org

[3]Department of Earth and Planetary Science, University of California, Berkeley, California 94720, USA

Annu. Rev. Earth Planet. Sci. 2019. 47:275–303

The *Annual Review of Earth and Planetary Sciences* is online at earth.annualreviews.org

https://doi.org/10.1146/annurev-earth-053018-060136

Keywords

climate change, ocean acidification, anoxia, extinction selectivity, physiology

Abstract

Flood basalts were Earth's largest volcanic episodes that, along with related intrusions, were often emplaced rapidly and coincided with environmental disruption: oceanic anoxic events, hyperthermals, and mass extinction events. Volatile emissions, both from magmatic degassing and vaporized from surrounding rock, triggered short-term cooling and longer-term warming, ocean acidification, and deoxygenation. The magnitude of biological extinction varied considerably, from small events affecting only select groups to the largest extinction of the Phanerozoic, with less-active organisms and those with less-developed respiratory physiology faring especially poorly. The disparate environmental and biological outcomes of different flood basalt events may at first order be explained by variations in the rate of volatile release modulated by longer trends in ocean carbon cycle buffering and the composition of marine ecosystems. Assessing volatile release, environmental change, and biological extinction at finer temporal resolution should be a top priority to refine ancient hyperthermals as analogs for anthropogenic climate change.

- Flood basalts, the largest volcanic events in Earth history, triggered dramatic environmental changes on land and in the oceans.
- Rapid volcanic carbon emissions led to ocean warming, acidification, and deoxygenation that often caused widespread animal extinctions.

- Animal physiology played a key role in survival during flood basalt extinctions, with reef builders such as corals being especially vulnerable.
- The rate and duration of volcanic carbon emission controlled the type of environmental disruption and the severity of biological extinction.

INTRODUCTION

Flood basalts are a subset of large igneous provinces (LIPs), which are loosely defined geologic provinces comprising anomalous concentrations of igneous activity of specific geographic and temporal extent and are distinct from igneous associations in magmatic arcs or mid-ocean ridges (Coffin & Eldholm 1994). The terms flood basalt and LIP are often used interchangeably, although the former should be reserved for the extrusive component of an LIP. The intrusive component of LIPs commonly includes layered mafic intrusions; in many cases these are economically important sources of platinum group, copper-nickel, and/or siderophile element ores. **Table 1** lists a number of layered mafic intrusions and their corresponding flood basalt provinces. Many older layered mafic intrusions exposed at deeper crustal levels, such as the Precambrian Bushveld, Muskox, Kiglapait, and Stillwater Complexes, lack a complementary extrusive flood basalt component that has presumably been eroded away.

Strictly speaking, many so-called flood basalt provinces contain lavas that are not basalt by geochemical criteria; andesites, dacites, and even rhyolites are often present, as are their alkali counterparts, but all these are generally present in minor proportions. The generally dominant basaltic lavas are most commonly tholeiitic in composition, being relatively enriched in silicon dioxide and impoverished in the incompatible elements such as the alkalis (e.g., sodium, potassium, and rubidium).

Flood basalts represent significant fluxes of mass and heat from Earth's mantle to the surface. The volume of erupted lava in some cases exceeds 2×10^6 km^3, with aerial footprints up to 10×10^6 km^2. Local accumulations of tens to hundreds of lava flows may exceed 4 km in stratigraphic succession. Within the stratigraphy of flood basalts, interbedded sediments are relatively rare although locally important, particularly near the fringes of the thickest lava accumulations. Increasingly, geochronology is revealing that flood basalts are emplaced on short geologic timescales, with the majority of lava extrusion occurring within less than 1–2 Ma. In some cases, flood basalts appear to have been erupted episodically in several rapid pulses (e.g., Knight et al. 2004).

Recognition of the brevity of main eruptive activity on such large spatial scales has led to increasing recognition of flood basalt events as posing potentially catastrophic perturbations on

Table 1 Layered mafic intrusions and genetically related flood basalt provinces

Layered mafic intrusion	Flood basalt	Location	Age
Skaergard Complex	North Atlantic	Greenland, United Kingdom, Denmark	Paleogene
Dufek Complex	Karoo-Ferrar	Antarctica, southern Africa	Jurassic
Freetown Complex	Central Atlantic	West Africa, Southwest Europe, South America, North America	Triassic/Jurassic
Noril'sk-Talnakh Suite	Siberian Traps	Siberia	Permian/Triassic
Duluth Complex	Keweenawan	North Central United States	Proterozoic

Earth's surficial environs—the atmosphere, hydrosphere, and cryosphere, and, consequently, the biosphere. Hypotheses linking flood basalt events to environmental crises have existed for decades and famously include the proposal by McLean (1980) that the Deccan Traps of modern India were the cause of the iconic mass extinction at the Cretaceous–Paleogene boundary. [We note that many flood basalt provinces are termed traps after the Swedish word *trappa* (stairs) in reference to the typical stairstep morphology of flood basalt outcrops] McLean's hypothesis failed to gain wide acceptance among Earth scientists for two main reasons: (*a*) The timing of the Deccan Traps eruption, and to a lesser extent that of the extinction, was poorly constrained, and (*b*) the discovery of a bolide impact stratigraphically coincident with the extinction provided an alternative explanation (Alvarez et al. 1980). In ensuing decades, geochronology applied to both flood basalts and mass extinctions has revitalized the case for a linkage between the Deccan Traps and the Cretaceous–Paleogene extinction and has clearly established a more general pattern of coincidence.

It is now clear that many flood basalt eruptions triggered extinction events ranging in magnitude from small crises to the largest extinctions of the Phanerozoic (Bond & Wignall 2014, Courtillot & Renne 2003) (**Figure 1**). The end-Permian and end-Triassic mass extinctions are

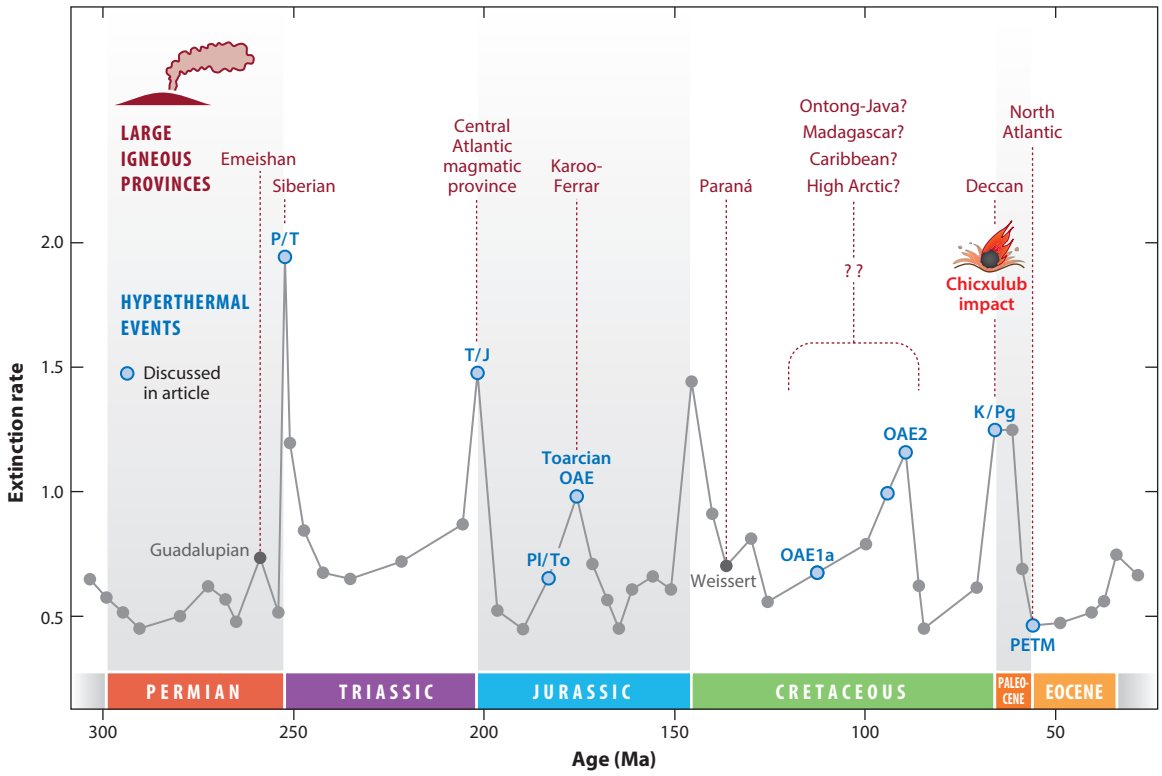

Figure 1

Marine invertebrate extinction rates (three-timer method, calculated from Paleobiology Database data at **http://fossilworks.org**) showing major and minor extinctions—Guadalupian, P/T, T/J, Pl/To, and K/Pg—OAEs, and the PETM hyperthermal. Events depicted by blue points are discussed in more detail in the text. These events aligned with flood basalt eruptions listed at the top (the exact igneous provinces corresponding to Cretaceous OAEs are uncertain) and, in the case of the K/Pg extinction, the Chicxulub meteorite impact. Abbreviations: K/Pg, end-Cretaceous; OAE, oceanic anoxic event; PETM, Paleocene–Eocene Thermal Maximum; Pl/To, Pliensbachian–Toarcian; P/T, end-Permian; T/J, end-Triassic.

the most notable examples where biosphere-wide taxonomic losses were contemporaneous with flood basalt eruption (Greene et al. 2012b, Payne & Clapham 2012). However, the Late Devonian mass extinction (Racki et al. 2018) and smaller extinctions such as the Guadalupian, Toarcian [a two-phase event with pulses at the Pliensbachian–Toarcian boundary and during the early Toarcian oceanic anoxic event (OAE)], and Cenomanian–Turonian also likely coincided with LIPs. The end-Cretaceous mass extinction also occurred during eruption of the Deccan Traps (Renne et al. 2015, Schoene et al. 2015), but its biotic effects are complicated and perhaps overshadowed by the contemporaneous Chicxulub impact event (Schulte et al. 2010).

Environmental disruption from LIPs was not limited to mass extinction events; other episodes of major paleoenvironmental change appear to have been coincident with flood basalt eruptions (**Figure 1**). Mesozoic OAEs, although typically exhibiting minor taxonomic losses or narrower biotic crises confined to particular groups (e.g., Erba 1994), may also have had a similar volcanic trigger to the larger mass extinctions (Kuroda et al. 2007, Turgeon & Creaser 2008). Finally, early Cenozoic hyperthermals—times of rapid temperature increase such as the Paleocene–Eocene Thermal Maximum (PETM)—share similarities with late Paleozoic/early Mesozoic extinctions and mid-Mesozoic OAEs (Gutjahr et al. 2017, McInerney & Wing 2011). The PETM caused ecological shifts, but taxonomic losses were negligible in most groups, with extinction confined to organisms such as calcareous nannoplankton and deep-sea benthic foraminifera (Gibbs et al. 2006, Thomas 2007). Although the source of carbon (C) released during the PETM is debated, a primarily volcanic origin is plausible (Gutjahr et al. 2017) and the event occurred at the same time as a major eruptive pulse in the North Atlantic magmatic province (Storey et al. 2007).

These hyperthermals, OEAs, and mass extinctions initially appeared to be disparate phenomena and even lack a collective term to refer to this type of event (we use hyperthermal to refer to all, for simplicity). More recently, however, geochemical proxy records are converging on a similar sequence of environmental disruption, including initial carbon dioxide (CO_2) release that triggered climate warming, decreased ocean pH, and potentially decreased carbonate saturation state, with subsequent weathering feedbacks leading to nutrient loading (eutrophication) and expansion of low-oxygen zones in the ocean. However, despite the hyperthermals sharing a common history, the specific patterns of environmental change differed dramatically among them, and the mechanisms by which LIP eruptions led to different types of events remain an outstanding question. Why were some events characterized by extensive anoxia and widespread black shale deposition whereas other events were dominated by warming and acidification?

Some of the largest mass extinctions were associated with hyperthermals, but not all hyperthermal events triggered widespread biotic losses. However, the link between LIP area and extinction severity is weak (Bond & Wignall 2014), and it remains unclear how environmental change during hyperthermals is translated into species extinctions. What factors can explain the highly variable biotic severity among hyperthermal events? Furthermore, what were the most important environmental kill mechanisms responsible for eliminating marine and terrestrial organisms? Species extinction and survival were likely rooted in their physiological responses to temperature, pH, oxygen, and related stressors, and a growing understanding from extant organisms provides clues to understand biotic vulnerability during hyperthermals.

In this review we focus on a range of past hyperthermals, including those that caused substantial extinction (end-Permian and end-Triassic mass extinctions), events with minor to moderate extinction (Pliensbachian–Toarcian boundary event, early Toarcian OAE, and Cenomanian–Turonian OAE2), and those with negligible or restricted biotic losses (Aptian OAE1a and the PETM). All these events coincided with flood basalt eruptions, although constraints on precise timing, magnitude, rate, and relationships among environmental changes continue to be refined. These are also not the only hyperthermals to have caused global upheaval; additional Eocene

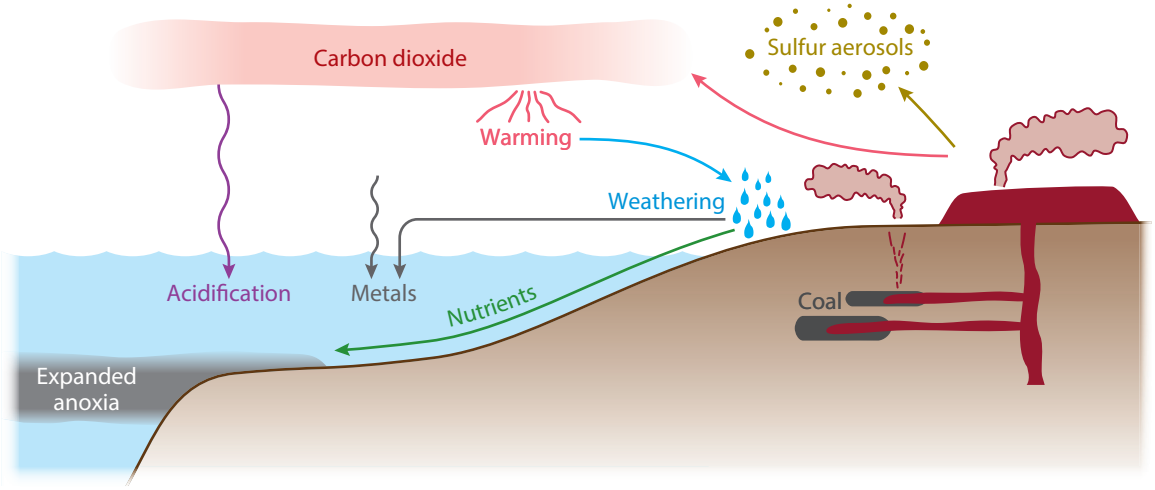

Figure 2

Selected environmental perturbations arising from flood basalt eruptions and related intrusive activity. Carbon dioxide and sulfur aerosols are sourced from both magmatic degassing and pyrogenic volatiles derived from rocks, especially coals, surrounding intrusive bodies. Subsequent perturbations include short-term cooling from aerosols and longer-term warming, ocean acidification, mercury and heavy metal deposition, an enhanced hydrologic cycle and weathering, and expanded anoxia resulting from eutrophication by weathering-derived nutrients.

hyperthermals, the Valanginian Weissert event, and others also perturbed the climate system. Despite those caveats, the varied nature of these events provides opportunities to generate a synthetic understanding of how flood basalt eruptions cause environmental disruption and biological extinction.

ENVIRONMENTAL DISRUPTION

Flood basalt eruptions triggered widespread environmental disruption in both terrestrial and marine ecosystems (**Figure 2**). On land, emission of sulfur dioxide (SO_2) aerosols would likely have caused short-term cooling following each eruption (Schmidt et al. 2016), with longer-term warming from CO_2. Other volatiles, such as hydrogen chloride and organohalogens, may have contributed to degradation of the ozone layer (Beerling et al. 2007). Plant and animal communities would have been further stressed not only by warming but also by shifts in the hydrologic cycle (Carmichael et al. 2017). Although the terrestrial record of ecological change is well known for the PETM, we focus here primarily on the marine record because extinctions and ecological changes are better documented in that setting for a range of hyperthermal events.

Decreased pH and Carbonate Saturation (Ocean Acidification)

Proxy data—for example, from plant stomata, pedogenic carbonates, or C isotopic composition of plant material—indicate geologically rapid increases in atmospheric partial pressure of carbon dioxide (pCO_2) levels coincident with LIPs (Barclay et al. 2010, McElwain 1999, McElwain et al. 2005, Schaller et al. 2011). This CO_2, which derives from ^{13}C-depleted magmatic, organic, and methane sources, is partially taken up by dissolving into the surface ocean, causing a negative C isotope excursion at most events (Jenkyns 2010, Korte & Kozur 2010, Kuroda et al. 2007,

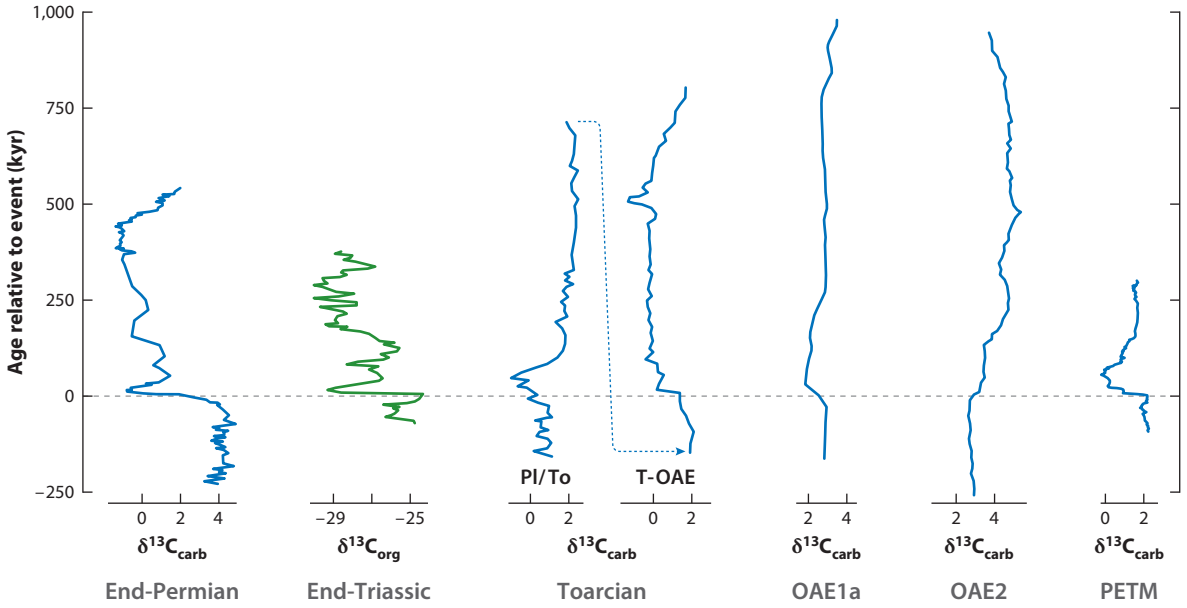

Figure 3

Comparison of C isotope records for the end-Permian (Burgess et al. 2017), end-Triassic (Xu et al. 2017), and Toarcian (Huang & Hesselbo 2014) events and the Aptian OAE1a (Malinverno et al. 2010), Cenomanian OAE2 (Clarkson et al. 2018), and PETM (Penman et al. 2016). The Toarcian event contains two phases (Pl/To boundary and early T-OAE), so the continuous C isotope curve is broken into two sections. The end-Triassic record is based on organic C, but all others are carbonate C isotopes. All records are shown at the same temporal and isotope scale. Abbreviations: C, carbon; OAE, oceanic anoxic event; PETM, Paleocene–Eocene Thermal Maximum; Pl/To, Pliensbachian–Toarcian; T-OAE, Toarcian oceanic anoxic event.

Ruhl et al. 2011) (**Figure 3**). In most cases the negative excursion initiated the hyperthermal and was followed by a gradual recovery to near-initial values, but in Cenomanian OAE2 the shift was predominantly a positive excursion, perhaps with negative phases within it (Kuroda et al. 2007). Despite diagenesis and local oceanographic conditions that can complicate the interpretation of C isotope records (Bachan et al. 2012, Schobben et al. 2017), isotope records provide strong support for C injection as a trigger of hyperthermals. However, the magnitude and especially rate of CO_2 release are much more difficult to constrain; the larger extinctions may have featured increases in atmospheric pCO_2 of two to four times (McElwain 1999, McElwain et al. 2005, Schaller et al. 2011), with somewhat smaller increases at OAE events (Barclay et al. 2010).

Uptake of CO_2 by the ocean mitigates the increase in atmospheric pCO_2 but can lead to potentially harmful shifts in ocean pH and saturation state as carbonic acid formed from dissolved CO_2 dissociates to generate protons and reduce carbonate ion concentration. Ocean acidification has often been invoked at past hyperthermals because of decreased carbonate sedimentation or extinction of hypercalcifying organisms, but these lines of argument, although suggestive, are not as strong as direct geochemical proxy evidence (Hönisch et al. 2012). Although surface-ocean pH likely decreased during all events, pH changes have reliably been reconstructed, using boron isotopes, for only the PETM (Penman et al. 2014) (**Figure 4**). A boron isotope excursion during the end-Permian mass extinction is consistent with acidification (Clarkson et al. 2015) but is based on bulk-rock measurements and does not coincide with a C isotope excursion or the extinction peak, so it needs confirmation from additional localities.

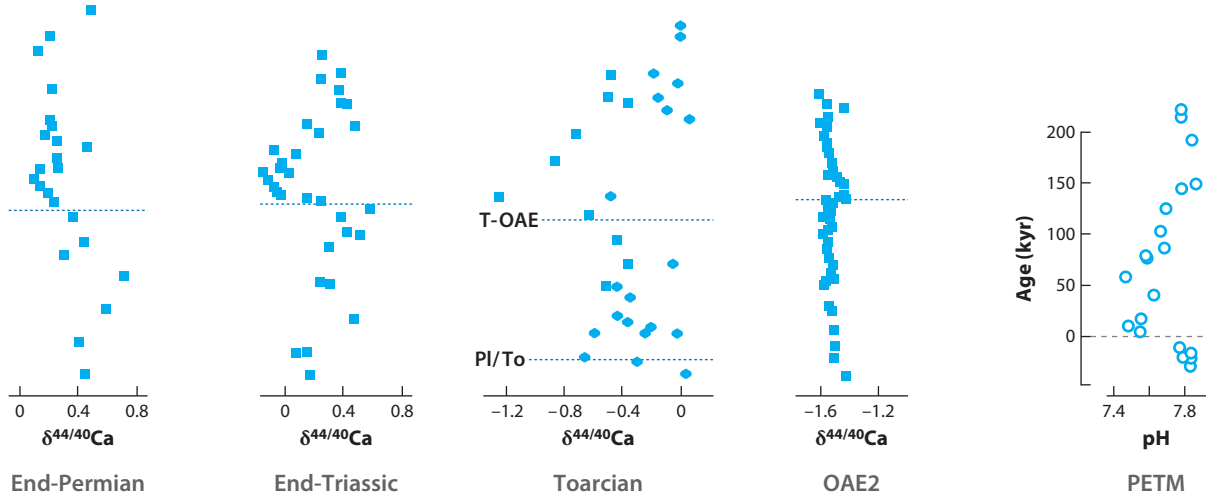

Figure 4

Comparison of pH- and carbonate saturation-related proxy data. Ca isotopes for the end-Permian (Silva-Tamayo et al. 2018), end-Triassic (Jost et al. 2017a), and Toarcian (Brazier et al. 2015) events and the Cenomanian OAE2 (Du Vivier et al. 2015), with bulk rock (*squares*) and brachiopods (only Toarcian) (*ovals*). The pH record for the PETM is based on boron isotopes (Penman et al. 2014). All Ca isotope records are shown at the same isotopic scale, but only the PETM record is time scaled. Abbreviations: Ca, calcium; OAE, oceanic anoxic event; PETM, Paleocene–Eocene Thermal Maximum; Pl/To, Pliensbachian–Toarcian; T-OAE, Toarcian oceanic anoxic event.

While surface-ocean pH is closely coupled with pCO_2, carbonate saturation state is highly sensitive to the rate of CO_2 release (Hönisch et al. 2012). As a result, true ocean acidification, featuring both decreased pH and decreased carbonate saturation, may not have occurred at all hyperthermal events. Saturation state changes also must be a short-lived phenomenon, lasting less than a few tens of kiloyears, and require very rapid rates of CO_2 release (Hönisch et al. 2012). The PETM again contains the strongest evidence for decreased surface-ocean saturation, thanks to the rich deep-sea record; carbonate dissolution indicates shoaling of the lysocline (the depth at which waters become undersaturated) in response to decreased carbonate ion concentration in surface waters (Zachos et al. 2005). Older events lack evidence from the deep sea, so most studies have used calcium (Ca) isotopes in an attempt to reconstruct the saturation decrease from reduced carbonate precipitation, increased dissolution of marine carbonates, or changes in isotope fractionation in response to decreased carbonate ion content (Brazier et al. 2015, Du Vivier et al. 2015, Jost et al. 2017a, Silva-Tamayo et al. 2018) (**Figure 4**). However, the complexity of the Ca cycle and isotope system, which includes influences from weathering, hydrothermal inputs, and local and global shifts in the mineralogy of carbonate precipitates in addition to saturation state, complicates interpretation. Despite those caveats, modeling of Ca isotope excursions could be consistent with decreased carbonate saturation at the end-Permian, end-Triassic, and Toarcian extinctions (Brazier et al. 2015, Jost et al. 2017a, Komar & Zeebe 2016, Silva-Tamayo et al. 2018), but evidence for saturation changes at Cretaceous OAEs is more equivocal (Blättler et al. 2011, Du Vivier et al. 2015). Saturation crises were also followed by overshoots in saturation state during the recovery interval, suggested by overdeepening of the carbonate compensation depth at the PETM (Penman et al. 2016) and perhaps by carbonate fans and other precipitates immediately after the end-Permian and end-Triassic extinctions (Greene et al. 2012a, Kershaw 2017).

Increased Temperature

Elevated atmospheric CO_2 associated with LIPs should lead to warming, both on land and in the oceans, with the strongest evidence typically coming from marine proxy records. Marine paleotemperature reconstructions imply substantial warming at hyperthermals, from only 2–4°C or less during Cretaceous OAEs to as much as 10°C across the end-Permian extinction (Forster et al. 2007, Korte et al. 2009, Naafs & Pancost 2016, Schobben et al. 2014, Suan et al. 2008, Sun et al. 2012, Zachos et al. 2003) (**Figure 5**).

However, marine paleotemperatures based on oxygen isotopes of biogenic material are also influenced by the oxygen isotope composition of seawater, adding uncertainty to estimates when changes in the hydrologic cycle are probable (Schobben et al. 2014). All proxies have complications and require careful application, but the use of multiple proxies, including magnesium/Ca ratios or TEX_{86} (based on lipids from cell membranes), provides independent evidence to support warming at Cretaceous and Cenozoic hyperthermals (Forster et al. 2007, Naafs & Pancost 2016, Zachos et al. 2003) (**Figure 5**). Multiple proxies also help distinguish true signals from diagenesis, but diagenetic alteration remains a risk with any proxy measurement. For example, many Toarcian paleotemperature estimates have been obtained from oxygen isotope measurements on belemnite cephalopod calcite, but it is now recognized that belemnite rostra were highly porous during life, potentially leading to isotopic alteration during diagenesis (Hoffmann et al. 2016). However, similar warming patterns appear in oxygen isotope records from brachiopods (Suan et al. 2008), providing more confidence in the proxy reconstructions.

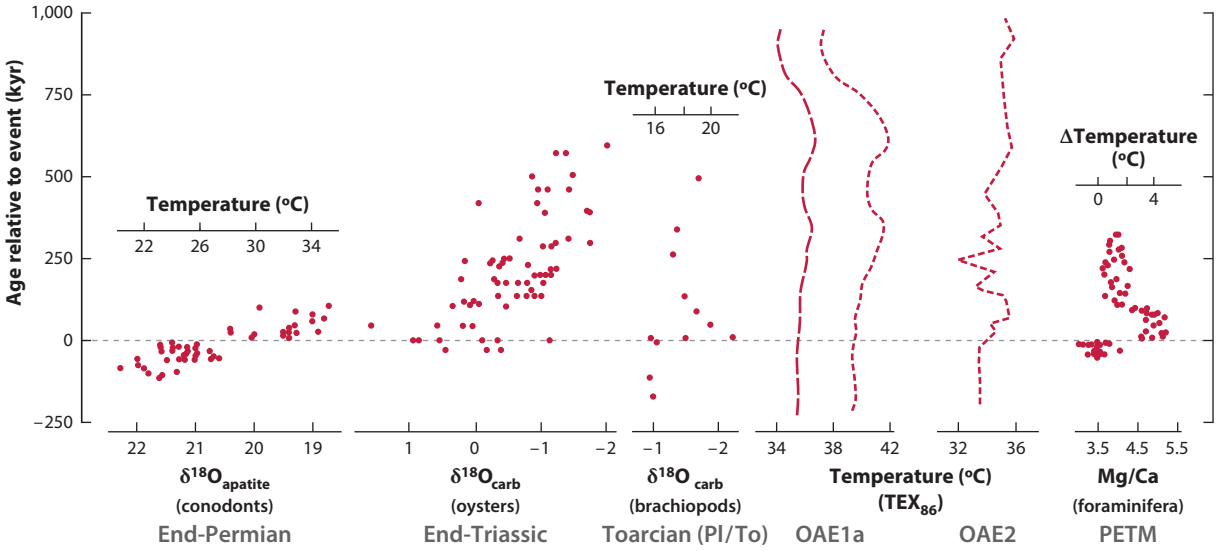

Figure 5

Comparison of proxy data for paleotemperature changes using conodont apatite O isotopes for the end-Permian event (Sun et al. 2012), oyster calcite O isotopes for the end-Triassic event (Korte et al. 2009), brachiopod O isotopes for the Toarcian event (Pl/To event only) (Suan et al. 2008), TEX_{86} (two different calibrations) for Aptian OAE1a (Naafs & Pancost 2016), TEX_{86} for Cenomanian OAE2 (Forster et al. 2007), and planktic foraminifera Mg/Ca for the PETM (Penman et al. 2014). The PETM Mg/Ca record shows temperature anomalies, but all others show absolute temperature estimates when provided. All records are shown at the same temporal and temperature scale. Abbreviations: Ca, calcium; Mg, magnesium; O, oxygen; OAE, oceanic anoxic event; PETM, Paleocene–Eocene Thermal Maximum; Pl/To, Pliensbachian–Toarcian; TEX_{86}, TetraEther indeX.

There are still unresolved issues of timing, particularly in older hyperthermals where proxy records come primarily from continental shelf sediments. For example, at the Triassic/Jurassic boundary, oxygen isotopes of oyster shells suggest long-term warming in the aftermath of the extinction but do not resolve any temperature change in the latest Triassic at the probable time of extinction itself (Korte et al. 2009). If warming occurred in the latest Triassic, as implied by a sharp C isotope excursion and terrestrial proxy data for increased pCO_2, it may have been below the resolution of the stratigraphic section or obscured by noise in the oxygen isotope record. Nonetheless, there is strong support for ocean warming, likely of small magnitude during Cretaceous OAEs, larger magnitude at the PETM and Pliensbachian–Toarcian boundary, and largest magnitude during the end-Permian extinction.

Low-Oxygen Conditions

Low-oxygen indicators were among the first signals of environmental disruption during hyperthermals to be recognized, in some cases even before the hypothesized connection with a flood basalt eruption. Sedimentological indicators, such as laminated and organic-rich shales with small-sized pyrite framboids, suggest deposition under locally anoxic conditions, particularly around the Permian/Triassic boundary and during Mesozoic OAEs (Bond & Wignall 2010, Schlanger & Jenkyns 1976, Wignall & Hallam 1992). Organic biomarkers further indicate local development of photic-zone euxinia (free hydrogen sulfide in surface waters), not only at the end-Permian extinction but even during the end-Triassic extinction and PETM when black shales were not as widely developed (Grice et al. 2005, Sluijs et al. 2014, van de Schootbrugge et al. 2013).

During these events, low-oxygen conditions were spatially patchy and temporally variable, but uranium isotope and other proxies for the global extent of anoxic waters indicate substantial expansions of anoxia (Brennecka et al. 2011, Clarkson et al. 2018, Dickson et al. 2012, Jost et al. 2017b). Reduced oxygen solubility and greater biological oxygen demand in warmer water played roles, but deoxygenation was driven primarily by nutrient loading that led to eutrophication and expansion of oxygen-minimum zones (Algeo et al. 2011, Meyer et al. 2008, Ostrander et al. 2017, Trabucho Alexandre et al. 2010). Ultimately, nutrient loading resulted from feedbacks during climate warming, a consequence of riverine phosphorus and other nutrient elements delivered by enhanced silicate weathering, as suggested by changes in the silica cycle (Corsetti et al. 2015, Penman 2016) and tracers such as osmium isotopes (Bottini et al. 2012, Dickson et al. 2015, Percival et al. 2016) and lithium isotopes (Pogge von Strandmann et al. 2013, Sun et al. 2018).

Mercury Loading

Hyperthermals were characterized by spikes in sedimentary mercury concentrations (Grasby et al. 2017, Percival et al. 2015, Scaife et al. 2017, Thibodeau et al. 2016). Elevated mercury content resulted in part from atmospheric deposition from volcanic sources (Grasby et al. 2017, Thibodeau et al. 2016), particularly in offshore environments, but mercury isotopes reveal a strong additional contribution from biomass or soil sources in coastal sediments (Grasby et al. 2017). However, the link between sedimentary mercury levels and the dissolved concentration in the surface ocean is complicated, in part because adsorption by organic matter is only one sink for dissolved mercury and the relative importance of different pathways under changing environmental conditions is uncertain (Lamborg et al. 2014). The effects of gaseous mercury escape to the atmosphere and the efficiency of organic-matter adsorption are difficult to predict, but Sanei et al. (2012) proposed that extreme mercury loading during the end-Permian extinction actually outpaced removal by organic-matter adsorption, exacerbating the buildup of dissolved concentrations. Despite

complexities of the mercury cycle, modern dissolved concentrations have increased due to anthropogenic emissions (Lamborg et al. 2014), so it is plausible that surface-ocean dissolved mercury concentrations also were elevated during past hyperthermals.

Although dissolved mercury concentrations likely were higher during hyperthermals, it is methylated mercury (methyl- and dimethylmercury), rather than the inorganic forms, that bioaccumulates and is a neurotoxin (Lamborg et al. 2014). Therefore, mercury is a potential contributor to extinctions if methylated mercury concentrations were also elevated. Methylation of mercury occurs in the sediments and in the water column, likely associated with bacterial remineralization of organic matter in both settings. In coastal sediments, mercury supply may be the limiting constraint on methylation, so higher sedimentary mercury concentrations could have led to greater diffusion of methylated mercury to the water column (Lamborg et al. 2014). However, greater dissolved sulfide in sediments, because of increased anoxia, may instead have changed mercury speciation and reduced rates of methylation (Lamborg et al. 2014). Although methylated mercury concentrations have increased along with anthropogenic mercury loading (Lamborg et al. 2014), processes governing methylation are not well understood and it is difficult to predict trends in methylated mercury across past hyperthermals.

PHYSIOLOGICAL MECHANISMS OF ENVIRONMENTAL STRESS

Extinctions associated with hyperthermal events, regardless of their size, had similar patterns of taxonomic and ecological selectivity. Selectivity patterns—for example, more severe extinctions among less-active, heavily calcified, or reef-building organisms (Clapham 2017, Clapham & Payne 2011, Kiessling & Simpson 2011, Knoll et al. 2007)—likely arose in part from variations in organism physiology that made certain groups more vulnerable to environmental changes during hyperthermals. Environmental changes may instead cause extinctions by altering the outcomes of species interactions (Gilman et al. 2010), although such indirect effects are difficult to predict or reconstruct from fossil assemblages or directly by reductions in individual organism performance. Attributing extinction of a single species to particular environmental stressors is also extremely challenging, but the scale of the fossil record provides opportunities to test for generalities in the biotic response to hyperthermal stressors. Furthermore, the existence of several extinctions associated with hyperthermals permits investigation of how organism physiology influences vulnerability to temperature stress, ocean acidification, deoxygenation, mercury loading, and other stressors.

Thermal and Respiratory Physiology

Temperature affects organisms across a range of biological scales, from the stability of individual molecules to whole-organism energy requirements. At molecular and cellular scales, heat stress alters cell membrane properties and damages protein folding, impairing cellular function and causing death if heat stress is severe (Richter et al. 2010). Organisms can mitigate this acute stress by inducing a heat-shock response to help repair or destroy misfolded proteins, restore the functioning of cell membranes, and maintain metabolic performance. The heat-shock response can help organisms cope with seasonal extreme temperatures in a rapidly warming world but is less suitable as a solution to frequent or prolonged high temperatures because production of heat-shock proteins requires expenditure of energy that could otherwise be used for growth, reproduction, or other activities.

While acute heat stresses can be lethal, increased temperatures may begin to have important effects on species survival by reducing whole-organism metabolic performance (Pörtner et al. 2017). Organisms must live within a metabolic energy budget, where some is allocated to baseline

maintenance needs (the basal or standard metabolic rate) with the remainder up to the organism's maximum metabolic rate available for growth, reproduction, feeding, movement, and other needs (the organism's aerobic scope) (Sokolova 2013). Among ectothermic organisms, which include nearly all marine invertebrates and fishes, an individual's standard metabolic rate increases with temperature, in large part due to greater rates of protein synthesis at higher temperatures and more-active ion transport to maintain ionic gradients across cell membranes (Clarke & Fraser 2004). These increased maintenance costs account for more of the total energy budget, and organisms may be able to only partially compensate with greater ventilation to increase gas exchange and faster circulation to supply more oxygen to the tissues (Pörtner et al. 2017). In the oxygen- and capacity-limited thermal tolerance (OCLTT) hypothesis, the mismatch between energy supply and demand becomes progressively more severe as temperatures increase beyond a threshold, reducing aerobic scope even before acute thresholds of the onset of anaerobic metabolism or protein stability are exceeded (Pörtner et al. 2017).

The OCLTT hypothesis therefore predicts that aerobic scope should be an important influence on survival during hyperthermals. However, oxygen supply does not constrain high-temperature performance in all ectotherms (Jutfelt et al. 2018). In addition, both metabolic rates and their scaling with temperature can be changed with acclimatization and longer-term evolutionary adaptation (Gunderson & Stillman 2015). Nevertheless, aerobic scope is typically greater in organisms with higher metabolic rates, suggesting that high metabolic rate should favor survival during hyperthermals if OCLTT is a widespread phenomenon.

Metabolic rate cannot be measured directly in extinct species, but generalizations on the basis of average activity levels of higher taxonomic groups support the prediction that more-active invertebrates were more likely to survive the end-Permian and end-Triassic extinctions (Clapham 2017). During the end-Permian extinction, this selectivity manifested in the severe extinction of sessile brachiopods, bryozoans, crinoids, and corals, compared to more moderate extinctions among gastropods, bivalves, and ostracods (Knoll et al. 2007, Payne & Clapham 2012). The smaller Toarcian extinction did not have a clear pattern of selectivity by activity level (Clapham 2017) but eliminated two orders of brachiopods (Vörös et al. 2016), a group that was especially vulnerable to earlier hyperthermals. However, the pattern is more equivocal when the analysis extends to include fishes. Sharks preferentially survived the end-Permian and end-Triassic extinctions, relative to invertebrates, whereas the extinction rate among bony actinopterygian fishes during the end-Triassic extinction was similar to the extinction of invertebrates (Vázquez & Clapham 2017). This may suggest limitations to the importance of aerobic scope during hyperthermals or confounding influences of other stressors and/or physiological vulnerabilities.

Preferential extinction of tropical organisms during some hyperthermals has been interpreted to result from warming (Kiessling et al. 2007), but the physiology of latitudinal vulnerability to high-temperature stress is complex. In some groups, tropical representatives face environmental temperatures closer to their upper thermal limit, but, at a broad scale, marine ectotherms have latitudinal range limits that closely follow their thermal tolerances (Sunday et al. 2012), suggesting that even temperate species will have populations living close to their thermal limit. However, temperate habitats are more variable over seasonal timescales, potentially conferring physiological resilience against longer-term environmental change compared to organisms that lived in more stable tropical habitats (Hofmann & Todgham 2010, Vinagre et al. 2016). Even though tropical habitats may undergo less warming than temperate regions, the exponential relationship between temperature and metabolic rate in ectotherms can cause metabolic oxygen demand to increase just as much or even more in tropical organisms (Dillon et al. 2010). In contrast, polar organisms may also be especially vulnerable to warming because many are adapted for stable, low-temperature habitats and may have narrow thermal tolerance windows and

acclimatization capacity (Peck et al. 2004, 2010; Sunday et al. 2011). Unfortunately, paleo-polar regions are scarce in the geological record, so there has been little investigation into whether those areas suffered disproportionate extinctions. Extinctions were severe at very high latitudes during the end-Permian crisis, perhaps more severe than at low-latitude Tethyan sites (Payne & Clapham 2012).

Although latitudinal extinction patterns need further investigation, with the possibility of tropical faunas being more severely affected during hyperthermals, there is stronger evidence for range shifts during ancient warming events (Reddin et al. 2018). Current anthropogenic warming has triggered ongoing range shifts on land and in the oceans, primarily by expansions at the poleward edge and contractions at the equatorial edge of species ranges (Lenoir & Svenning 2015). Ranges can be difficult to reconstruct from sparse fossil occurrences, but warm-water ammonites may have expanded poleward during the early Toarcian (Dera et al. 2011). Similarly, certain coccolithophores disappeared from equatorial regions at the PETM, as did coral reefs, and both groups became restricted to cooler habitats at mid- to high latitudes (Gibbs et al. 2016, Speijer et al. 2012). It is less clear whether tropical heating made low-latitude regions uninhabitable, even though the maximum thermal limits of marine organisms may be only a few degrees warmer than modern equatorial temperatures (Nguyen et al. 2011). The purported absence of Early Triassic vertebrate fossils from equatorial latitudes has been attributed to extreme temperatures after the end-Permian extinction (Sun et al. 2012), but as Early Triassic vertebrate localities are rare, this biogeographic pattern may not be reliable (Romano et al. 2017). Trends in planktic foraminifera and dinoflagellates are more robust because of those groups' abundances, and local disappearances from PETM equatorial sites could be consistent with thermal stress (Aze et al. 2014, Frieling et al. 2017).

Acid-Base Balance and Respiratory Physiology

Increased seawater pCO_2 and reduced pH could also have been important stressors during hyperthermals, acting on respiratory function and perhaps having synergistic effects with temperature (Pörtner et al. 2005). In animals, oxygen is transported from the gas-exchange organ (lungs or gills) to the tissues by pH-sensitive blood pigments such as hemoglobin, hemocyanin, and hemerythrin. The pH-dependent oxygen binding of blood pigments—called the Bohr effect—underpins their functioning but also makes blood pigments vulnerable to decreasing seawater pH, which reduces the amount of oxygen carried by the pigments unless the organism can maintain consistent blood pH through buffering systems. Although blood proteins can contribute limited buffering, active transport of bicarbonate ion, either from seawater or produced by hydration of metabolic CO_2, provides the most important buffer by raising blood alkalinity to maintain high pH even under increased blood pCO_2 levels (Melzner et al. 2009).

Paleontologists have invoked a broader concept of physiological buffering—a combination of metabolic rate, gas-exchange abilities, and calcification mechanisms—as a contributor to survival during past hyperthermals such as the end-Permian extinction (Clapham & Payne 2011, Kiessling & Simpson 2011, Knoll et al. 2007). Similar selectivity occurred at the Toarcian extinction but not at younger events such as Cenomanian–Turonian OAE2 or the PETM (Payne et al. 2016). Although these studies did not specifically address acid-base buffering, the preferential survival of more-active organisms raises the question of whether bicarbonate buffering capacity was important. Complete bicarbonate buffering tends to be found in active animals, including many fishes and crustaceans, with partial buffering in other crustaceans, cephalopods, and some echinoids (Collard et al. 2014, Melzner et al. 2009, Whiteley 2011). In contrast, bicarbonate buffering only minimally compensates for decreasing seawater pH in many less-active bivalves and other

echinoids (Collard et al. 2014, Heinemann et al. 2012, Michaelidis et al. 2005, Stapp et al. 2018). Despite the preferential survival of more-active organisms during past hyperthermals, there is not a clear signal of selectivity from bicarbonate buffering capacity. Both bivalves and cidaroid echinoids, which have minimal buffer capacity (Collard et al. 2014, Stapp et al. 2018), fared comparatively well during the end-Permian extinction, as did crustaceans with presumably high buffer capacity. However, little is known about the buffer capacity of paleontologically important organisms such as brachiopods, bryozoans, and crinoids. Furthermore, although bicarbonate buffering can be an important response to maintain respiratory function, the organism must expend energy to actively remove protons produced during the hydration of CO_2 to bicarbonate (Melzner et al. 2009). The additional costs from proton removal can force reallocation of energy away from other critical needs, such as growth or reproduction (Pan et al. 2015, Stumpp et al. 2012), potentially reducing species survival over many generations.

Marine animals must maintain a positive pCO_2 gradient, with higher levels in body fluids than in seawater, to drive diffusive CO_2 excretion from the body (Melzner et al. 2009). Active organisms tend to have body fluids with higher pCO_2 (Melzner et al. 2009), and, when body fluid pCO_2 is high and pH is low, increased seawater pCO_2 may have negligible effects on acid-base status (Collard et al. 2014). Selective survival of more-active groups at past hyperthermals, in particular the end-Permian extinction, is consistent with reduced vulnerability in groups that likely had higher pCO_2, although pCO_2 levels of body fluids are known for comparatively few animal groups. In the few measurements available for organisms typically characterized by paleontologists as poorly buffered (e.g., cnidarians, brachiopods), those animals appear to have lower pCO_2 than bivalves, gastropods, or crustaceans (Collip 1920).

Knoll et al. (2007) argued that organisms with better-developed gas-exchange structures were more likely to survive at the end-Permian extinction, but few other studies have evaluated the potential for selectivity within taxonomic groups because of gas-exchange ability. Active organisms tend to have more complex gas-exchange structures to remove CO_2 produced during exercise (Melzner et al. 2009). But even among organisms with similar ecology and morphology, such as echinoids, species with better-developed gas exchange may be able to more efficiently remove accumulated CO_2, thus reducing the need for high buffering capacity (Collard et al. 2013). It would be interesting to consider whether differences in lophophore type, the main gas-exchange organ in brachiopods, can account for differential survival among members of that group during the end-Permian, end-Triassic, and Toarcian extinctions. Ager (1987) suggested that rhynchonellide brachiopods may have preferentially survived because of their extensible lophophores, although in the context of feeding ecology rather than respiratory physiology.

During ocean acidification, organisms that cannot buffer extracellular pH or remove excess CO_2 through gas exchange will undergo respiratory acidosis and reductions in the oxygen capacity of blood pigments. It is not clear, however, whether animals with highly pH-sensitive pigments (a strong Bohr effect) will be more vulnerable. Knoll et al. (2007) speculated that ammonoid cephalopods may have experienced severe extinctions due to a strong Bohr effect, using the extreme Bohr effect of modern coleoid cephalopods (squid and relatives) as a model. However, it seems unlikely that ammonoids had respiratory pigments with squid-like Bohr effects. Extant squid support an extreme Bohr effect by having unusual respiratory physiology, probably involving oxygen uptake through the skin—a respiratory adaptation that likely was not present in externally shelled cephalopods (Pörtner 1995). The pH sensitivity of blood pigments appears to have little physiological signal and little relationship with metabolic rate or activity levels (Fabry et al. 2008), so it is uncertain whether differences in the Bohr effect among species would have caused predictable selectivity during past hyperthermals.

Hypoxia Tolerance

Ocean deoxygenation threatens marine animals by reducing oxygen availability and compromising aerobic metabolism (Deutsch et al. 2015, Diaz & Rosenberg 2008). Like other stressors, deoxygenation impacts the respiratory physiology of marine organisms, requiring adaptations to tolerate hypoxia, or reduced oxygen supply to tissues. Animals regulate metabolic demand when oxygen is plentiful and are able to reduce their oxygen demand in response to decreased environmental oxygen availability, but species with lower metabolic rates will be able to withstand lower oxygen levels before the onset of anaerobic metabolism and ultimately death (Seibel 2011, Vaquer-Sunyer & Duarte 2011). Given this, active organisms such as fish and crustaceans tend to be more sensitive to hypoxia, whereas mollusks, echinoderms, and cnidarians can tolerate lower oxygen levels (Vaquer-Sunyer & Duarte 2011). However, motile organisms also can employ behavioral strategies to avoid low-oxygen waters (Chu & Tunnicliffe 2015), so expanded oxygen-minimum zones may have reduced available habitat area for only some groups, which is unlikely to cause significant extinctions unless the reductions were extreme.

Global patterns of extinction selectivity at ancient hyperthermals were not consistent with hypoxic stress, as more-active organisms tended to be more, not less, likely to survive (Clapham 2017, Knoll et al. 2007). However, local development of dysoxic, anoxic, or euxinic conditions had profound effects on community composition (Danise et al. 2013). Communities in anoxic basins were dominated by flat clams, such as species of *Claraia* following the end-Permian extinction, *Pseudomytiloides* and *Bositra* during the Toarcian extinction, and the inoceramid *Mytiloides* during Cenomanian OAE2 (Danise et al. 2013, Harries & Little 1999, Petsios & Bottjer 2016). Among foraminifera, species with thin shells and high surface area became more abundant during Cenomanian OAE2 (Kaiho & Hasegawa 1994). These foraminifera and bivalve species plausibly had hypoxia-tolerant physiological adaptations, including large surface areas for gas exchange, allowing them to colonize low-oxygen habitats when most other organisms were excluded. Tolerance of hypoxia is further enhanced by the ability to increase ventilation or blood circulation and, in animals, the presence of blood pigments with high oxygen affinity (the ability to bind oxygen at low concentrations) and large pH sensitivity (Seibel 2011). Organisms with these traits should have fared better during hyperthermals in which deoxygenation was widespread, but it may not be feasible to identify which extinct species could greatly elevate ventilation rates or had high-affinity blood pigments.

Although deoxygenation did not clearly result in taxonomic selectivity at a global scale, expansion of oxygen-minimum zones predicts that extinctions should have been more intense in offshore habitats. Onshore-offshore patterns of extinction selectivity have received little study, and reconstructing depositional environment from literature compilations is challenging, but there is little evidence for disproportionate extinction of offshore or slope-dwelling species. Kiessling et al. (2007) found that end-Triassic extinction rates instead were significantly lower in offshore habitats, and Chen et al. (2011) also argued for preferential survival of offshore and slope brachiopod faunas in South China during the end-Permian extinction. Deep-water benthic foraminifera suffered extinction at the PETM, but abyssal habitats would not have been affected by expansion of mid-water OMZs, and the widespread survival of ostracod crustaceans in the same habitats is inconsistent with hypoxia (Foster et al. 2013, Thomas 2007).

Water-column deoxygenation is likely to impact burrowing organisms more severely because the subsurface redox boundary will occur at shallower depths in the sediment (Diaz & Rosenberg 2008). The preferential extinction of infaunal bivalves during the Toarcian extinction (Aberhan & Baumiller 2003) and a shift toward epifauna-dominated communities during Cenomanian OAE2 (Harries & Little 1999) were consistent with hypoxia stress, and extinction rates were also higher

among infaunal bivalves than epifaunal species during the end-Triassic extinction (Kiessling et al. 2007, McRoberts & Newton 1995). Clapham & Payne (2011) found that epifauna preferentially survived, after accounting for mineralogy and physiological buffering, but this analysis included gastropods as well as bivalves in the epifaunal group. Given consistent selectivity within bivalves across several events, it is therefore possible that deoxygenation influenced extinction patterns within taxonomic groups but perhaps either did not impart selectivity at broader taxonomic scales or had effects that were overwhelmed by other stressors.

Calcification Physiology

The coincidence between extinction and CO_2 release suggests that calcification could be a vulnerability of shelly organisms. Virtually all marine calcifying organisms form their shells from a seawater reservoir that is modified to varying degrees, primarily by active ion pumping to remove hydrogen ions and increase the pH of calcifying fluids. Although a decreased saturation state is only tentatively inferred at some hyperthermals, reduced pH during these events still could have impaired calcification because more acidic conditions would increase the energy required to pump hydrogen ions out of calcifying fluids (Comeau et al. 2018, Ries 2011). In experiments, calcification responses vary among groups but decrease at lower saturation states and lower pH (Ries et al. 2009), even though in nature some species can calcify in undersaturated waters and the cost of mineral precipitation is a minor component of shell formation (Spalding et al. 2017). Shell formation is aided in most marine calcifiers by modifications to the composition of their calcifying fluid, providing some resistance to ocean acidification, although at an energetic cost (Comeau et al. 2018, de Nooijer et al. 2009, Ries 2011).

Organisms with carbonate shells were less likely to survive the end-Permian and end-Triassic extinctions (Clapham & Payne 2011, Hautmann et al. 2008), consistent with stress from pH and/or saturation state changes. However, the noncalcifying comparison group is quite heterogeneous with long-ranging taxa, including siliceous sponges, phosphatic brachiopods, and phosphatic conulariids. Some studies have also interpreted preferential extinction of aragonitic bivalves (Hautmann et al. 2008, Kiessling et al. 2007) as a signal of ocean acidification (Hautmann et al. 2008), but bivalves, like many other calcifiers, control polymorph mineralogy with an organic template and modulate calcifying fluid chemistry to aid in precipitation. In contrast, carbonate polymorph was not a significant predictor of survival during the end-Permian extinction (Clapham & Payne 2011). Severe end-Permian extinctions of groups such as brachiopods and corals have been partly attributed to their weak control over calcification (Clapham & Payne 2011, Knoll et al. 2007), but living corals heavily modify the chemistry of calcifying fluids (Comeau et al. 2018), and some living brachiopods also can maintain shell growth and repair during acidification experiments (Cross et al. 2016). At the PETM, calcification of benthic foraminifera actually increased rather than decreased (Foster et al. 2013), and there is only limited evidence for calcification stress in calcareous nannofossils (Gibbs et al. 2016, Raffi et al. 2009).

Although the degree to which calcification stresses influenced survival is uncertain for many groups, hyperthermals were often associated with calcification crises in reef ecosystems (Kiessling & Simpson 2011). Heavily calcified reef builders suffered disproportionately severe extinction during the end-Permian (Clapham & Payne 2011, Knoll et al. 2007), end-Triassic (Hautmann et al. 2008, Kiessling et al. 2007), and Toarcian extinctions (Lathuilière & Marchal 2009). Hyperthermals also caused significant reductions in reef volume, even in events such as the PETM where taxonomic losses were not elevated (Kiessling & Simpson 2011), in some cases leading to reef gaps where reefs constructed from animal skeletons were rare (Martindale et al. 2019). Given the spatial correspondence between modern reef-building corals and water with high saturation

state, it is plausible that reduced pH and saturation contributed to sponge or coral extinctions and accompanying reef crises. This suggests that reef-building organisms are particularly vulnerable to hyperthermal events.

Mercury Toxicity

Sedimentary mercury concentrations indicate high rates of mercury delivery to surface waters during hyperthermals from runoff and atmospheric deposition (Grasby et al. 2017), but the contribution of mercury toxicity to extinction is far less clear. Toxic methylated mercury perhaps increased, by analogy with the modern, but controls on methylation are poorly understood (Lamborg et al. 2014) and there are no direct constraints on changes during hyperthermals. However, even if methylated mercury levels increased substantially, they likely contributed little to observed patterns of extinction. Methylated mercury becomes increasingly concentrated in animals at higher trophic levels, so its neurotoxic effects would be stronger in top predators (Lamborg et al. 2014) and minimal in grazing, suspension-feeding, and deposit-feeding invertebrates that compose most of the fossil record.

Selective extinctions from mercury neurotoxicity should preferentially eliminate species with high trophic positions, but there is little evidence for this pattern. Sharks suffered little extinction during the end-Permian, end-Triassic, and Toarcian extinctions, and, while end-Triassic extinction rates were elevated among bony fish, extinctions were no more severe than among benthic invertebrates (Vázquez & Clapham 2017). The PETM did not alter fish community structure (Sibert et al. 2016), although a potential extinction not seen in the fossil record has been proposed on the basis of molecular phylogenetics (Arcila & Tyler 2017). However, ichthyosaurs were likely among the top predators in Mesozoic oceans and suffered major extinction between the Late Triassic and Early Jurassic (Fischer et al. 2014, Thorne et al. 2011). These losses were plausibly driven by the end-Triassic hyperthermal, but the precise timing of ichthyosaur extinctions is difficult to resolve. In contrast, the Toarcian OAE did not trigger extinctions among ichthyosaurs (Maxwell & Vincent 2016), but the group's final disappearance in the late Cenomanian was likely associated with environmental disruptions during OAE2 (Fischer et al. 2016).

Synergistic Stressors

The interlinked nature of environmental disruptions following LIP eruptions (**Figure 2**) would have exposed organisms to multiple stressors during past hyperthermals rather than simply to changing temperature, pH, or oxygen in isolation (Gibbs et al. 2016, Knoll et al. 2007, Pietsch et al. 2014, Song et al. 2015). The severity of environmental change can also be modulated by interactions between co-occurring stressors, such as the effects of temperature on dissolved oxygen levels. Multiple stressors can have synergistic impacts at the physiological scale as well. For example, high temperatures increase an organism's oxygen demand and reduce its aerobic scope, while lower pH may reduce the oxygen-carrying capacity of blood pigments and seasonal hypoxia can reduce oxygen availability (Pörtner et al. 2005). Likewise, temperature can have variable effects on susceptibility to metal pollution, and metal pollution can in turn reduce thermal tolerance (Sokolova & Lannig 2008). As such, a focus on identifying individual kill mechanisms is probably misplaced, but ancient hyperthermals provide multiple exceptional case studies to investigate the organismal response to multistressor environmental disruption in natural ecosystems over evolutionary timescales.

The synergistic effects of multiple stressors are best integrated in an energy budget framework (Sokolova 2013). Temperature, pH, and oxygen all influence metabolic supply and demand and,

therefore, the amount of energy available for growth, reproduction, movement, and other activities necessary for survival of the species. In many cases organisms are able to maintain some aspects of biological function—for example, maintaining calcification rates despite lower pH levels—but at an energetic cost that may force trade-offs with other processes. However, the need for trade-offs can be minimized if greater food supply provides additional energy to support extra regulatory costs (Thomsen et al. 2013). In all these cases, the effects of environmental stressors, the interactions among stressors, and the mitigation from greater food supply are nuanced and variable among species. Nevertheless, the combined impact of multistressor global change during hyperthermals is fundamentally an energy budget problem.

THE IMPORTANCE OF RATE

C emission rates would have strongly influenced both the nature and the severity of environmental and biological disruption during hyperthermals. Similarly, the rate of SO_2 aerosol emission would have played a critical role in the severity and frequency of short-term cooling events in terrestrial ecosystems. Over longer timescales, C cycle feedbacks can mitigate the severity of warming or ocean acidification if the tempo of C release is slower than the timescale of those feedbacks. Likewise, organisms may be able to adapt to a changing environment if the rate of that change is slow. However, direct assessment of the rate of environmental change on decadal to centennial timescales relevant for biological adaptation is rarely feasible in ancient hyperthermals (Kemp et al. 2015) due to the episodic nature of sediment deposition and hiatuses as well as postdepositional mixing of sediments by bioturbation. Moreover, these timescales are below the resolution of relevant geochronometers, thus hindering linkages between such environmental effects and their possible relationships to volcanic forcing events.

Two main C sources attributable to LIPs are magmatic volatiles exsolved from magma itself and pyrogenic volatiles released by degassing of crustal materials in contact with the magma. Magmatic volatile releases to the atmosphere are estimated to include as much as 1 gigaton/year of both SO_2 and CO_2 during eruptions (Black & Manga 2017, Jones et al. 2016, Self et al. 2005). Pyrogenic volatiles may yield comparable amounts of these species depending on the nature of crustal materials intruded by the magma (Black et al. 2012; McElwain et al. 2005; Svensen et al. 2004, 2009). These two sources blur together when pyrogenic volatiles are absorbed by undersaturated magma only to be exsolved later during decompression as envisaged by Black & Manga (2017).

The environmental impacts of LIP-derived volatiles depend strongly on the tempo of input to the atmosphere (Black & Manga 2017, Schmidt et al. 2016, Self et al. 2014), particularly for S, which has an effective timescale of decades. As such, it is commonly assumed that the eruptive flux of lavas is a proxy for the flux of volatiles to the atmosphere. In principle this is determinable insofar as a stratigraphic sequence of lavas provides a geologic record, but unfortunately the frequency of individual eruptions is generally too high to be resolved by available dating methods.

However, there is clear evidence that both magmatic and pyrogenic volatiles may be released into the atmosphere before eruption (Edmonds & Wallace 2017) in so-called passive emissions. Passive emission may be especially important for pyrogenic volatiles, as is believed to be the case when Siberian Traps magmas intruded coal beds in Permo-Triassic time, possibly accounting for the majority of CO_2 released. Intrusion into coal beds has also been invoked at the end-Triassic and Toarcian extinctions. In such cases, the record of intrusion emplacement may provide the best estimate of the tempo of atmospheric CO_2 loading (Burgess et al. 2017, Davies et al. 2017, McElwain et al. 2005). Unfortunately, the record of intrusions is generally obscured by the fact that some are inevitably unexposed.

The total amount of climate-modifying gases released into the atmosphere by LIPs and the tempo at which they are released are not well constrained. A key question remains about the relative importance of pyrogenic versus magmatic origin of these gases; if the former is dominant, then the environmental effects of LIPs should vary significantly depending on the nature of crustal materials into which they are emplaced. In the case of CO_2, it is widely accepted that biogenic C (i.e., from sediments) is an important contributor due to the common occurrence of negative C isotope anomalies coincident with mass extinctions (**Figure 3**). However, Black et al. (2014) found that the Siberian Traps contain S with isotopic composition similar to that of mid-ocean ridge basalts, suggesting relatively minor contribution from sedimentary sources.

Rates of Acclimatization and Adaptation

Organisms may be able to tolerate environmental changes if they have sufficient capacity to acclimatize over short timescales or if they are able to adapt through evolution over multiple generations. Acclimatization occurs during the lifetime of an individual organism, reflecting phenotypic plasticity and the ability to shift its environmental tolerances. In some organisms, plasticity is limited (Gunderson & Stillman 2015), but transgenerational plasticity—nongenetic changes that shift environmental tolerances from parent to offspring—may also increase resilience (Munday 2014, Ross et al. 2016). Adaptation, via genetic evolution, can be rapid and thus enable organisms to survive environmental change (Lohbeck et al. 2014, Pespeni et al. 2013), but the limits on adaptive potential remain unclear (Kelly & Hofmann 2013, Sunday et al. 2014).

Acclimatization and adaptation have not been reconstructed for fossil species during ancient hyperthermals, but the occurrence of elevated extinction rates indicates that adaptive potential can be overwhelmed if environmental disruption is sufficiently rapid and/or severe. The rate of environmental change presumably played a key role because slower change both reduces the need for acclimatization and provides more time for genetic evolution to shift an organism's tolerances. Organisms likely also were more vulnerable if the magnitude of environmental change was large over decade to century timescales relevant for evolutionary adaptation.

Feedbacks Can Mitigate or Enhance Environmental Disruption

The rate of environmental change can be reduced by feedbacks, such as silicate weathering to remove CO_2 from the atmosphere or shoaling of the lysocline to buffer oceanic pH and saturation state. However, these feedbacks operate slowly, over thousands to hundreds of thousands of years, and so can meaningfully reduce the rate of environmental change only if the C perturbation is also slow. The effectiveness of C cycle feedbacks likely also varied among different hyperthermals. More recent hyperthermals, such as Cretaceous OAEs or the PETM, would have been better buffered against pH and saturation changes because the oceanic C cycle was stabilized by the large deep-sea reservoir of carbonate sediments present following the mid-Mesozoic evolution of planktic organisms (Ridgwell & Zeebe 2005). In contrast, the C and climate system would have been more susceptible to large perturbations during the end-Triassic and especially end-Permian extinctions. The physical location of the LIP itself may also have influenced the magnitude of feedbacks because mafic rocks contribute disproportionately to CO_2 drawdown by silicate weathering, and weathering rates are considerably higher in the tropics (Dessert et al. 2003, Jagoutz et al. 2016). As a result, CO_2 drawdown may have been more rapid following the end-Triassic extinction because of tropical weathering of Central Atlantic magmatic province volcanics, whereas the higher-latitude Siberian Traps may have led to a more muted weathering feedback following the end-Permian extinction.

Other feedbacks could instead have enhanced the magnitude of local environmental change, such as the impact of weathering and nutrient supply on anoxia. Hyperthermals were characterized by enhanced chemical weathering and likely also by intensification of the hydrological cycle, supplying more nutrients that would drive eutrophication and expanded anoxia in shallow waters (Carmichael et al. 2017, Pogge von Strandmann et al. 2013). The prevalence of anoxia may have been further enhanced by continental configurations and oceanic circulation that favored nutrient trapping (Meyer et al. 2008, Trabucho Alexandre et al. 2010).

LARGE IGNEOUS PROVINCES AND EXTINCTIONS: A SYNTHETIC CLASSIFICATION

Although LIP magmatic activity almost certainly triggered environmental change, why did the nature of that environmental change differ among events, and why did only some events cause severe and widespread extinctions? The rate of volatile emission, and therefore the rate of environmental disruption, likely provided a first-order constraint (Rothman 2017).

The end-Permian extinction, end-Triassic extinction, Pliensbachian–Toarcian boundary event, and PETM likely represented hyperthermal events with very rapid rates of C release, creating sharp negative C isotope excursions and environmental changes dominated by warming and perhaps acidification (**Figure 6**). Anoxic waters expanded, but black shale deposition was not as widespread as at true OAE events, likely because C release exceeded a critical threshold only for a shorter duration. At the other end of the spectrum, the early Toarcian OAE, Aptian OAE1a, and Cenomanian OAE2 may have been characterized by more gradual C release but over long timescales, which promoted widespread anoxia and resulting black shale deposits through weathering feedbacks. C isotope excursions were shallowly negative or even positive, most likely because the positive isotopic shift from enhanced organic burial counterbalanced the injection of isotopically negative C (Kump & Arthur 1999). These events also had more muted temperature and, probably, pH changes than other events due to feedbacks mitigating environmental disruption.

Extinction severity corresponded roughly, but not entirely, with the inferred rate of environmental disruption. The end-Permian and end-Triassic events were both mass extinctions, but the Pliensbachian–Toarcian boundary was a smaller event, and the PETM exhibited only limited extinction. However, the early Toarcian OAE and Cenomanian OAE2 were also minor extinctions but were more substantial crises than the PETM, despite having more muted C isotope excursions. Direct measures of high-resolution rates of environmental change are unattainable for these ancient events, so it is possible that some Mesozoic OAEs contained shorter intervals (decades to centuries) of very rapid change despite their overall more drawn-out appearance. The fact that not all rapid events triggered substantial extinctions may point to magnitude as a secondary control. The magnitude of end-Permian and end-Triassic environmental changes, as inferred from proxy records, was considerably larger than the Pliensbachian–Toarcian or PETM, indicating that rapid rates of change were sustained for longer or that extinction severity increased as adaptive limits were reached in more organisms.

Long-term changes in the Earth system, such as the evolution of planktic calcifying organisms, also influenced the rate and severity of hyperthermals. The mid-Mesozoic shift to a more stabilized oceanic C cycle (Ridgwell & Zeebe 2005) may also have reduced the likelihood of catastrophic environmental disruption, particularly dampening fluctuations in pH and saturation state. Although the sample size is small, the only post-Jurassic hyperthermal to trigger even moderate extinction was Cenomanian OAE2, while most pre-Cretaceous hyperthermals were associated with extinctions.

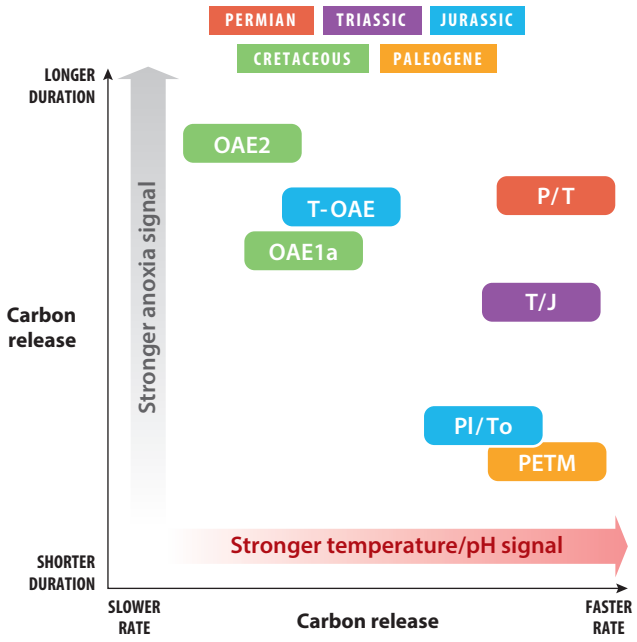

Figure 6

Schematic classification of hyperthermal events on the basis of rate and duration of C emissions, as qualitatively inferred from C cycle and paleotemperature proxy records. We propose that events with faster C injection tend to show a stronger signal of temperature increase and probably ocean pH change, whereas longer-duration events are characterized by extensive black shales. Events of very large magnitude, with both faster rate and longer duration, include mass extinctions such as the P/T and T/J. The Pl/To event and PETM have extremely similar proxy records and so are plotted separately for visibility only. Abbreviations: C, carbon; OAE, oceanic anoxic event; PETM, Paleocene–Eocene Thermal Maximum; Pl/To, Pliensbachian–Toarcian; P/T, end-Permian, T/J, end-Triassic; T-OAE, Toarcian oceanic anoxic event.

The end-Cretaceous mass extinction was a severe and rapid (at least in the shallow marine realm) event that coincided with not only the Deccan Traps but also the Chicxulub impact, so the exact influence of volcanically driven environmental change is unclear. It is clear that significant warming in marine (Barnet et al. 2018) and terrestrial (Tobin et al. 2014) environments began about 300 kyr before the impact and extinction, coincident with the inception of main Deccan volcanism. Thus, it is possible that the subsequent cooling at the end-Cretaceous period (Barnet et al. 2018, Tobin et al. 2014) provided critical stress to ecosystems that were adapting to the preceding warming event. The relative contributions of volcanism versus impact of C burial to the cooling event remain unclear. The initial recovery of marine ecosystems after the extinction was delayed until the waning of Deccan volcanism, suggesting that volcanism played at least a suppressing role in the recovery (Renne et al. 2015).

Finally, successive hyperthermal extinctions, which preferentially removed more vulnerable organisms such as brachiopods and crinoids, resulted in marine ecosystems dominated by more-active organisms that would have been better able to withstand these environmental stressors (Bambach et al. 2002, Clapham 2017). In a sense, each hyperthermal extinction may have hardened ecosystems to be less vulnerable to future events. Nevertheless, more sensitive groups that remained, such as reef-building corals, were among the few groups to suffer during the PETM and remain vulnerable to temperature and ocean acidification.

FUTURE DIRECTIONS

The coincidence between flood basalt eruptions and extinctions, OAEs, and other hyperthermals is becoming increasingly clear, but there are still many unresolved issues. We suggest that variations in the rate of volatile emission can provide a first-order framework for unifying these seemingly disparate events. However, further testing of this framework and a more nuanced explanation of the differences among events will require more precise radioisotopic age constraints on the rates of eruption and of intrusive emplacement. The contribution of magmatic versus pyrogenic (typically coal-derived) gas emissions, particularly for CO_2, should also be refined to extrapolate emission rates from radioisotopically dated lavas and intrusions.

On the biological side, more high-resolution studies of extinction timing and tempo are needed, especially for events other than the end-Permian extinction, to assess the coincidence of taxonomic losses and environmental disruption. Likewise, patterns of extinction selectivity, which are important for testing physiological hypotheses and linking these to specific environmental triggers, have mostly been documented for the end-Permian, end-Triassic, and Toarcian extinctions. Even though other events were small, studies targeting Cretaceous OAEs and the PETM will yield a more complete picture of the severity and selectivity of hyperthermal extinctions. This is particularly true for taxonomic groups such as crustaceans and echinoids, which became much more abundant in the Cretaceous and Cenozoic.

Finally, ancient hyperthermals can provide a range of analogs for anthropogenic climate change, but bridging the divide between broadscale but low temporal and taxonomic resolution paleontological studies and narrowly focused but high-resolution biological studies is paramount. The fossil record provides exceptional scale to assess biotic change over multiple events, at evolutionary timescales, and in natural ecosystems, but more work is required to develop proxies for physiological traits of extinct species and to assess organismal responses at timescales relevant for ongoing global change.

DISCLOSURE STATEMENT

The authors are not aware of any affiliations, memberships, funding, or financial holdings that might be perceived as affecting the objectivity of this review.

ACKNOWLEDGMENTS

The authors are grateful to innumerable colleagues who have contributed to their knowledge over the years and to the funding agencies (National Science Foundation, National Geographic Society, Esper Larsen Fund, and Ann and Gordon Getty Foundation) that have enabled them to investigate the topic of this review. An anonymous reviewer provided helpful suggestions to improve the clarity of this review.

LITERATURE CITED

Aberhan M, Baumiller TK. 2003. Selective extinction among Early Jurassic bivalves: a consequence of anoxia. *Geology* 31:1077–80

Ager DV. 1987. Why the rhynchonellid brachiopods survived and the spiriferids did not: a suggestion. *Palaeontology* 30:853–57

Algeo TJ, Chen ZQ, Fraiser ML, Twitchett RJ. 2011. Terrestrial–marine teleconnections in the collapse and rebuilding of Early Triassic marine ecosystems. *Palaeogeogr. Palaeoclimatol. Palaeoecol.* 308:1–11

Alvarez LW, Alvarez W, Asaro F, Michel HV. 1980. Extraterrestrial cause for the Cretaceous-Tertiary extinction. *Science* 208:1095–108

Arcila D, Tyler JC. 2017. Mass extinction in tetraodontiform fishes linked to the Palaeocene–Eocene thermal maximum. *Proc. R. Soc. B* 284:20171771

Aze T, Pearson PN, Dickson AJ, Badger MPS, Bown PR, et al. 2014. Extreme warming of tropical waters during the Paleocene–Eocene Thermal Maximum. *Geology* 42:739–42

Bachan A, van de Schootbrugge B, Fiebig J, McRoberts CA, Ciarapica G, Payne JL. 2012. Carbon cycle dynamics following the end-Triassic mass extinction: constraints from paired $\delta^{13}C_{carb}$ and $\delta^{13}C_{org}$ records. *Geochem. Geophys. Geosystems* 13:Q09008

Bambach RK, Knoll AH, Sepkoski JJ. 2002. Anatomical and ecological constraints on Phanerozoic animal diversity in the marine realm. *PNAS* 99:6854–59

Barclay RS, McElwain JC, Sageman BB. 2010. Carbon sequestration activated by a volcanic CO_2 pulse during Ocean Anoxic Event 2. *Nat. Geosci.* 3:205–8

Barnet JSK, Littler K, Kroon D, Leng MJ, Westerhold T, et al. 2018. A new high-resolution chronology for the late Maastrichtian warming event: establishing robust temporal links with the onset of Deccan volcanism. *Geology* 46:147–50

Beerling DJ, Harfoot M, Lomax B, Pyle JA. 2007. The stability of the stratospheric ozone layer during the end-Permian eruption of the Siberian Traps. *Philos. Trans. R. Soc. A* 365:1843–66

Black BA, Elkins-Tanton LT, Rowe MC, Peate IU. 2012. Magnitude and consequences of volatile release from the Siberian Traps. *Earth Planet. Sci. Lett.* 317–318:363–73

Black BA, Hauri EH, Elkins-Tanton LT, Brown SM. 2014. Sulfur isotopic evidence for sources of volatiles in Siberian Traps magmas. *Earth Planet. Sci. Lett.* 394:58–69

Black BA, Manga M. 2017. Volatiles and the tempo of flood basalt magmatism. *Earth Planet. Sci. Lett.* 458:130–40

Blättler CL, Jenkyns HC, Reynard LM, Henderson GM. 2011. Significant increases in global weathering during Oceanic Anoxic Events 1a and 2 indicated by calcium isotopes. *Earth Planet. Sci. Lett.* 309:77–88

Bond DPG, Wignall PB. 2010. Pyrite framboid study of marine Permian–Triassic boundary sections: a complex anoxic event and its relationship to contemporaneous mass extinction. *Geol. Soc. Am. Bull.* 122:1265–79

Bond DPG, Wignall PB. 2014. Large igneous provinces and mass extinctions: an update. In *Volcanism, Impacts, and Mass Extinctions: Causes and Effects*, ed. G Keller, AC Kerr, pp. 29–55. Geol. Soc. Am. Spec. Pap. 505. Boulder, CO: Geol. Soc. Am.

Bottini C, Cohen AS, Erba E, Jenkyns HC, Coe AL. 2012. Osmium-isotope evidence for volcanism, weathering, and ocean mixing during the early Aptian OAE 1a. *Geology* 40:583–86

Brazier J-M, Suan G, Tacail T, Simon L, Martin JE, et al. 2015. Calcium isotope evidence for dramatic increase of continental weathering during the Toarcian oceanic anoxic event (Early Jurassic). *Earth Planet. Sci. Lett.* 411:164–76

Brennecka GA, Herrmann AD, Algeo TJ, Anbar AD. 2011. Rapid expansion of oceanic anoxia immediately before the end-Permian mass extinction. *PNAS* 108:17631–34

Burgess SD, Muirhead JD, Bowring SA. 2017. Initial pulse of Siberian Traps sills as the trigger of the end-Permian mass extinction. *Nat. Commun.* 8:164

Carmichael MJ, Inglis GN, Badger MPS, Naafs BDA, Behrooz L, et al. 2017. Hydrological and associated biogeochemical consequences of rapid global warming during the Paleocene-Eocene Thermal Maximum. *Glob. Planet. Change* 157:114–38

Chen J, Chen Z-Q, Tong J. 2011. Environmental determinants and ecologic selectivity of benthic faunas from nearshore to bathyal zones in the end-Permian mass extinction: brachiopod evidence from South China. *Palaeogeogr. Palaeoclimatol. Palaeoecol.* 308:84–97

Chu JWF, Tunnicliffe V. 2015. Oxygen limitations on marine animal distributions and the collapse of epibenthic community structure during shoaling hypoxia. *Glob. Change Biol.* 21:2989–3004

Clapham ME. 2017. Organism activity levels predict marine invertebrate survival during ancient global change extinctions. *Glob. Change Biol.* 23:1477–85

Clapham ME, Payne JL. 2011. Acidification, anoxia, and extinction: a multiple logistic regression analysis of extinction selectivity during the Middle and Late Permian. *Geology* 39:1059–62

Clarke A, Fraser KPP. 2004. Why does metabolism scale with temperature? *Funct. Ecol.* 18:243–51

Clarkson MO, Kasemann SA, Wood RA, Lenton TM, Daines SJ, et al. 2015. Ocean acidification and the Permo-Triassic mass extinction. *Science* 348:229–32

Clarkson MO, Stirling CH, Jenkyns HC, Dickson AJ, Porcelli D, et al. 2018. Uranium isotope evidence for two episodes of deoxygenation during Oceanic Anoxic Event 2. *PNAS* 115:2918–23

Coffin MF, Eldholm O. 1994. Large igneous provinces: crustal structure, dimensions, and external consequences. *Rev. Geophys.* 32:1–36

Collard M, Dery A, Dehairs F, Dubois P. 2014. Euechinoidea and Cidaroidea respond differently to ocean acidification. *Comp. Biochem. Physiol. A* 174:45–55

Collard M, Laitat K, Moulin L, Catarino AI, Grosjean P, Dubois P. 2013. Buffer capacity of the coelomic fluid in echinoderms. *Comp. Biochem. Physiol. A* 166:199–206

Collip JB. 1920. The alkali reserve of marine fish and invertebrates: the excretion of carbon dioxide. *J. Biol. Chem.* 44:329–44

Comeau S, Cornwall CE, De Carlo TM, Krieger E, McCulloch MT. 2018. Similar controls on calcification under ocean acidification across unrelated coral reef taxa. *Glob. Change Biol.* 24:4857–68

Corsetti FA, Ritterbush KA, Bottjer DJ, Greene SE, Ibarra Y, et al. 2015. Investigating the paleoecological consequences of supercontinent breakup: Sponges clean up in the Early Jurassic. *Sediment. Record* 13(2):4–10

Courtillot VE, Renne PR. 2003. On the ages of flood basalt events. *C. R. Geosci.* 335:113–40

Cross EL, Peck LS, Lamare MD, Harper EM. 2016. No ocean acidification effects on shell growth and repair in the New Zealand brachiopod *Calloria inconspicua* (Sowerby, 1846). *ICES J. Mar. Sci.* 73:920–26

Danise S, Twitchett RJ, Little CTS, Clémence M-E. 2013. The impact of global warming and anoxia on marine benthic community dynamics: an example from the Toarcian (Early Jurassic). *PLOS ONE* 8:e56255

Davies JHFL, Marzoli A, Bertrand H, Youbi N, Ernesto M, Schaltegger U. 2017. End-Triassic mass extinction started by intrusive CAMP activity. *Nat. Commun.* 8:15596

de Nooijer LJ, Toyofuku T, Kitazato H. 2009. Foraminifera promote calcification by elevating their intracellular pH. *PNAS* 106:15374–78

Dera G, Neige P, Dommergues J-L, Brayard A. 2011. Ammonite paleobiogeography during the Pliensbachian–Toarcian crisis (Early Jurassic) reflecting paleoclimate, eustasy, and extinctions. *Glob. Planet. Change* 78:92–105

Dessert C, Dupré B, Gaillardet J, François LM, Allègre CJ. 2003. Basalt weathering laws and the impact of basalt weathering on the global carbon cycle. *Chem. Geol.* 202:257–73

Deutsch C, Ferrel A, Seibel B, Portner H-O, Huey RB. 2015. Climate change tightens a metabolic constraint on marine habitats. *Science* 348:1132–35

Diaz RJ, Rosenberg R. 2008. Spreading dead zones and consequences for marine ecosystems. *Science* 321:926–29

Dickson AJ, Cohen AS, Coe AL. 2012. Seawater oxygenation during the Paleocene-Eocene Thermal Maximum. *Geology* 40:639–42

Dickson AJ, Cohen AS, Coe AL, Davies M, Shcherbinina EA, Gavrilov YO. 2015. Evidence for weathering and volcanism during the PETM from Arctic Ocean and Peri-Tethys osmium isotope records. *Palaeogeogr. Palaeoclimatol. Palaeoecol.* 438:300–7

Dillon ME, Wang G, Huey RB. 2010. Global metabolic impacts of recent climate warming. *Nature* 467:704–6

Du Vivier ADC, Jacobson AD, Lehn GO, Selby D, Hurtgen MT, Sageman BB. 2015. Ca isotope stratigraphy across the Cenomanian–Turonian OAE 2: links between volcanism, seawater geochemistry, and the carbonate fractionation factor. *Earth Planet. Sci. Lett.* 416:121–31

Edmonds M, Wallace PJ. 2017. Volatiles and exsolved vapor in volcanic systems. *Elements* 13:29–34

Erba E. 1994. Nannofossils and superplumes: the Early Aptian "nannoconid crisis." *Paleoceanography* 9:483–501

Fabry VJ, Seibel BA, Feely RA, Orr JC. 2008. Impacts of ocean acidification on marine fauna and ecosystem processes. *ICES J. Mar. Sci.* 65:414–32

Fischer V, Bardet N, Benson RBJ, Arkhangelsky MS, Friedman M. 2016. Extinction of fish-shaped marine reptiles associated with reduced evolutionary rates and global environmental volatility. *Nat. Commun.* 7:10825

Fischer V, Cappetta H, Vincent P, Garcia G, Goolaerts S, et al. 2014. Ichthyosaurs from the French Rhaetian indicate a severe turnover across the Triassic–Jurassic boundary. *Naturwissenschaften* 101:1027–40

Forster A, Schouten S, Moriya K, Wilson PA, Sinninghe Damsté JS. 2007. Tropical warming and intermittent cooling during the Cenomanian/Turonian oceanic anoxic event 2: sea surface temperature records from the equatorial Atlantic. *Paleoceanography* 22:PA1219

Foster LC, Schmidt DN, Thomas E, Arndt S, Ridgwell A. 2013. Surviving rapid climate change in the deep sea during the Paleogene hyperthermals. *PNAS* 110:9273–76

Frieling J, Gebhardt H, Huber M, Adekeye OA, Akande SO, et al. 2017. Extreme warmth and heat-stressed plankton in the tropics during the Paleocene-Eocene Thermal Maximum. *Sci. Adv.* 3:e1600891

Gibbs SJ, Bown PR, Ridgwell A, Young JR, Poulton AJ, O'Dea SA. 2016. Ocean warming, not acidification, controlled coccolithophore response during past greenhouse climate change. *Geology* 44:59–62

Gibbs SJ, Bown PR, Sessa JA, Bralower TJ, Wilson PA. 2006. Nannoplankton extinction and origination across the Paleocene-Eocene Thermal Maximum. *Science* 314:1770–73

Gilman SE, Urban MC, Tewksbury J, Gilchrist GW, Holt RD. 2010. A framework for community interactions under climate change. *Trends Ecol. Evol.* 25:325–31

Grasby SE, Shen W, Yin R, Gleason JD, Blum JD, et al. 2017. Isotopic signatures of mercury contamination in latest Permian oceans. *Geology* 45:55–58

Greene SE, Bottjer DJ, Corsetti FA, Berelson WM, Zonneveld J-P. 2012a. A subseafloor carbonate factory across the Triassic-Jurassic transition. *Geology* 40:1043–46

Greene SE, Martindale RC, Ritterbush KA, Bottjer DJ, Corsetti FA, Berelson WM. 2012b. Recognising ocean acidification in deep time: an evaluation of the evidence for acidification across the Triassic-Jurassic boundary. *Earth-Sci. Rev.* 113:72–93

Grice K, Cao C, Love GD, Böttcher ME, Twitchett RJ, et al. 2005. Photic zone euxinia during the Permian-Triassic superanoxic event. *Science* 307:706–9

Gunderson AR, Stillman JH. 2015. Plasticity in thermal tolerance has limited potential to buffer ectotherms from global warming. *Proc. R. Soc. B* 282:20150401

Gutjahr M, Ridgwell A, Sexton PF, Anagnostou E, Pearson PN, et al. 2017. Very large release of mostly volcanic carbon during the Palaeocene–Eocene Thermal Maximum. *Nature* 548:573–77

Harries PJ, Little CT. 1999. The early Toarcian (Early Jurassic) and the Cenomanian–Turonian (Late Cretaceous) mass extinctions: similarities and contrasts. *Palaeogeogr. Palaeoclimatol. Palaeoecol.* 154:39–66

Hautmann M, Benton MJ, Tomašových A. 2008. Catastrophic ocean acidification at the Triassic-Jurassic boundary. *Neues Jahrb. Geol. Paläontol.* 249:119–27

Heinemann A, Fietzke J, Melzner F, Böhm F, Thomsen J, et al. 2012. Conditions of *Mytilus edulis* extracellular body fluids and shell composition in a pH-treatment experiment: acid-base status, trace elements and δ^{11}B. *Geochem. Geophys. Geosystems* 13:Q01005

Hoffmann R, Richter DK, Neuser RD, Jöns N, Linzmeier BJ, et al. 2016. Evidence for a composite organic–inorganic fabric of belemnite rostra: implications for palaeoceanography and palaeoecology. *Sediment. Geol.* 341:203–15

Hofmann GE, Todgham AE. 2010. Living in the now: physiological mechanisms to tolerate a rapidly changing environment. *Annu. Rev. Physiol.* 72:127–45

Hönisch B, Ridgwell A, Schmidt DN, Thomas E, Gibbs SJ, et al. 2012. The geological record of ocean acidification. *Science* 335:1058–63

Huang C, Hesselbo SP. 2014. Pacing of the Toarcian Oceanic Anoxic Event (Early Jurassic) from astronomical correlation of marine sections. *Gondwana Res.* 25:1348–56

Jagoutz O, Macdonald FA, Royden L. 2016. Low-latitude arc–continent collision as a driver for global cooling. *PNAS* 113:4935–40

Jenkyns HC. 2010. Geochemistry of oceanic anoxic events. *Geochem. Geophys. Geosystems* 11:Q03004

Jones MT, Jerram DA, Svensen HH, Grove C. 2016. The effects of large igneous provinces on the global carbon and sulphur cycles. *Palaeogeogr. Palaeoclimatol. Palaeoecol.* 441:4–21

Jost AB, Bachan A, van de Schootbrugge B, Brown ST, DePaolo DJ, Payne JL. 2017a. Additive effects of acidification and mineralogy on calcium isotopes in Triassic/Jurassic boundary limestones. *Geochem. Geophys. Geosystems* 18:113–24

Jost AB, Bachan A, van de Schootbrugge B, Lau KV, Weaver KL, et al. 2017b. Uranium isotope evidence for an expansion of marine anoxia during the end-Triassic extinction. *Geochem. Geophys. Geosystems* 18:3093–108

Jutfelt F, Norin T, Ern R, Overgaard J, Wang T, et al. 2018. Oxygen- and capacity-limited thermal tolerance: blurring ecology and physiology. *J. Exp. Biol.* 221:jeb169615

Kaiho K, Hasegawa T. 1994. End-Cenomanian benthic foraminiferal extinctions and oceanic dysoxic events in the northwestern Pacific Ocean. *Palaeogeogr. Palaeoclimatol. Palaeoecol.* 111:29–43

Kelly MW, Hofmann GE. 2013. Adaptation and the physiology of ocean acidification. *Funct. Ecol.* 27:980–90

Kemp DB, Eichenseer K, Kiessling W. 2015. Maximum rates of climate change are systematically underestimated in the geological record. *Nat. Commun.* 6:9890

Kershaw S. 2017. Palaeogeographic variation in the Permian–Triassic boundary microbialites: a discussion of microbial and ocean processes after the end-Permian mass extinction. *J. Palaeogeogr.* 6:97–107

Kiessling W, Aberhan M, Brenneis B, Wagner PJ. 2007. Extinction trajectories of benthic organisms across the Triassic–Jurassic boundary. *Palaeogeogr. Palaeoclimatol. Palaeoecol.* 244:201–22

Kiessling W, Simpson C. 2011. On the potential for ocean acidification to be a general cause of ancient reef crises. *Glob. Change Biol.* 17:56–67

Knight KB, Nomade S, Renne PR, Marzoli A, Bertrand H, Youbi N. 2004. The Central Atlantic Magmatic Province at the Triassic–Jurassic boundary: paleomagnetic and $^{40}Ar/^{39}Ar$ evidence from Morocco for brief, episodic volcanism. *Earth Planet. Sci. Lett.* 228(1):143–60

Knoll AH, Bambach RK, Payne JL, Pruss S, Fischer WW. 2007. Paleophysiology and end-Permian mass extinction. *Earth Planet. Sci. Lett.* 256:295–313

Komar N, Zeebe RE. 2016. Calcium and calcium isotope changes during carbon cycle perturbations at the end-Permian. *Paleoceanography* 31:115–30

Korte C, Hesselbo SP, Jenkyns HC, Rickaby REM, Spotl C. 2009. Palaeoenvironmental significance of carbon- and oxygen-isotope stratigraphy of marine Triassic–Jurassic boundary sections in SW Britain. *J. Geol. Soc.* 166:431–45

Korte C, Kozur HW. 2010. Carbon-isotope stratigraphy across the Permian–Triassic boundary: a review. *J. Asian Earth Sci.* 39:215–35

Kump LR, Arthur MA. 1999. Interpreting carbon-isotope excursions: carbonates and organic matter. *Chem. Geol.* 161:181–98

Kuroda J, Ogawa N, Tanimizu M, Coffin M, Tokuyama H, et al. 2007. Contemporaneous massive subaerial volcanism and late Cretaceous Oceanic Anoxic Event 2. *Earth Planet. Sci. Lett.* 256:211–23

Lamborg C, Bowman K, Hammerschmidt C, Gilmour C, Munson K, et al. 2014. Mercury in the Anthropocene ocean. *Oceanography* 27:76–87

Lathuilière B, Marchal D. 2009. Extinction, survival and recovery of corals from the Triassic to Middle Jurassic time. *Terra Nova* 21:57–66

Lenoir J, Svenning J-C. 2015. Climate-related range shifts—a global multidimensional synthesis and new research directions. *Ecography* 38:15–28

Lohbeck KT, Riebesell U, Reusch TBH. 2014. Gene expression changes in the coccolithophore *Emiliania huxleyi* after 500 generations of selection to ocean acidification. *Proc. R. Soc. B* 281:20140003

Malinverno A, Erba E, Herbert TD. 2010. Orbital tuning as an inverse problem: chronology of the early Aptian oceanic anoxic event 1a (Selli Level) in the Cismon APTICORE. *Paleoceanography* 25:PA2203

Martindale RC, Foster WJ, Velledits F. 2019. The survival, recovery, and diversification of metazoan reef ecosystems following the end-Permian mass extinction event. *Palaeogeogr. Palaeoclimatol. Palaeoecol.* 513:100–15

Maxwell EE, Vincent P. 2016. Effects of the early Toarcian Oceanic Anoxic Event on ichthyosaur body size and faunal composition in the Southwest German Basin. *Paleobiology* 42:117–26

McElwain JC. 1999. Fossil plants and global warming at the Triassic-Jurassic boundary. *Science* 285:1386–90

McElwain JC, Wade-Murphy J, Hesselbo SP. 2005. Changes in carbon dioxide during an oceanic anoxic event linked to intrusion into Gondwana coals. *Nature* 435:479–82

McInerney FA, Wing SL. 2011. The Paleocene-Eocene Thermal Maximum: a perturbation of carbon cycle, climate, and biosphere with implications for the future. *Annu. Rev. Earth Planet. Sci.* 39:489–516

McLean DM. 1980. Terminal Cretaceous catastrophe. *Nature* 287:760

McRoberts CA, Newton CR. 1995. Selective extinction among end-Triassic European bivalves. *Geology* 23:102–4

Melzner F, Gutowska MA, Langenbuch M, Dupont S, Lucassen M, et al. 2009. Physiological basis for high CO_2 tolerance in marine ectothermic animals: Pre-adaptation through lifestyle and ontogeny? *Biogeosciences* 6:2313–31

Meyer KM, Kump LR, Ridgwell A. 2008. Biogeochemical controls on photic-zone euxinia during the end-Permian mass extinction. *Geology* 36:747–50

Michaelidis B, Ouzounis C, Paleras A, Pörtner H. 2005. Effects of long-term moderate hypercapnia on acid-base balance and growth rate in marine mussels *Mytilus galloprovincialis*. *Mar. Ecol. Prog. Ser.* 293:109–18

Munday PL. 2014. Transgenerational acclimation of fishes to climate change and ocean acidification. *F1000Prime Rep.* 6:99

Naafs BDA, Pancost RD. 2016. Sea-surface temperature evolution across Aptian Oceanic Anoxic Event 1a. *Geology* 44:959–62

Nguyen KDT, Morley SA, Lai C-H, Clark MS, Tan KS, et al. 2011. Upper temperature limits of tropical marine ectotherms: global warming implications. *PLOS ONE* 6:e29340

Ostrander CM, Owens JD, Nielsen SG. 2017. Constraining the rate of oceanic deoxygenation leading up to a Cretaceous Oceanic Anoxic Event (OAE-2: ∼94 Ma). *Sci. Adv.* 3:e1701020

Pan T-CF, Applebaum SL, Manahan DT. 2015. Experimental ocean acidification alters the allocation of metabolic energy. *PNAS* 112:4696–701

Payne JL, Bush AM, Chang ET, Heim NA, Knope ML, Pruss SB. 2016. Extinction intensity, selectivity and their combined macroevolutionary influence in the fossil record. *Biol. Lett.* 12:20160202

Payne JL, Clapham ME. 2012. End-Permian mass extinction in the oceans: an ancient analog for the twenty-first century? *Annu. Rev. Earth Planet. Sci.* 40:89–111

Peck LS, Morley SA, Clark MS. 2010. Poor acclimation capacities in Antarctic marine ectotherms. *Mar. Biol.* 157:2051–59

Peck LS, Webb KE, Bailey DM. 2004. Extreme sensitivity of biological function to temperature in Antarctic marine species. *Funct. Ecol.* 18:625–30

Penman DE. 2016. Silicate weathering and North Atlantic silica burial during the Paleocene-Eocene Thermal Maximum. *Geology* 44:731–34

Penman DE, Hönisch B, Zeebe RE, Thomas E, Zachos JC. 2014. Rapid and sustained surface ocean acidification during the Paleocene-Eocene Thermal Maximum. *Paleoceanography* 29:357–69

Penman DE, Turner SK, Sexton PF, Norris RD, Dickson AJ, et al. 2016. An abyssal carbonate compensation depth overshoot in the aftermath of the Palaeocene–Eocene Thermal Maximum. *Nat. Geosci.* 9:575–80

Percival LME, Cohen AS, Davies MK, Dickson AJ, Hesselbo SP, et al. 2016. Osmium isotope evidence for two pulses of increased continental weathering linked to Early Jurassic volcanism and climate change. *Geology* 44:759–62

Percival LME, Witt MLI, Mather TA, Hermoso M, Jenkyns HC, et al. 2015. Globally enhanced mercury deposition during the end-Pliensbachian extinction and Toarcian OAE: a link to the Karoo–Ferrar Large Igneous Province. *Earth Planet. Sci. Lett.* 428:267–80

Pespeni MH, Sanford E, Gaylord B, Hill TM, Hosfelt JD, et al. 2013. Evolutionary change during experimental ocean acidification. *PNAS* 110:6937–42

Petsios E, Bottjer DJ. 2016. Quantitative analysis of the ecological dominance of benthic disaster taxa in the aftermath of the end-Permian mass extinction. *Paleobiology* 42:380–93

Pietsch C, Mata SA, Bottjer DJ. 2014. High temperature and low oxygen perturbations drive contrasting benthic recovery dynamics following the end-Permian mass extinction. *Palaeogeogr. Palaeoclimatol. Palaeoecol.* 399:98–113

Pogge von Strandmann PAE, Jenkyns HC, Woodfine RG. 2013. Lithium isotope evidence for enhanced weathering during Oceanic Anoxic Event 2. *Nat. Geosci.* 6:668–72

Pörtner H-O. 1995. Coordination of metabolism, acid-base regulation and haemocyanin function in cephalopods. *Mar. Freshw. Behav. Physiol.* 25:131–48

Pörtner H-O, Bock C, Mark FC. 2017. Oxygen- and capacity-limited thermal tolerance: bridging ecology and physiology. *J. Exp. Biol.* 220:2685–96

Pörtner H-O, Langenbuch M, Michaelidis B. 2005. Synergistic effects of temperature extremes, hypoxia, and increases in CO_2 on marine animals: from Earth history to global change. *J. Geophys. Res.* 110(C9):C09S10

Racki G, Rakociński M, Marynowski L, Wignall PB. 2018. Mercury enrichments and the Frasnian-Famennian biotic crisis: a volcanic trigger proved? *Geology* 46:543–46

Raffi I, Backman J, Zachos JC, Sluijs A. 2009. The response of calcareous nannofossil assemblages to the Paleocene Eocene Thermal Maximum at the Walvis Ridge in the South Atlantic. *Mar. Micropaleontol.* 70:201–12

Reddin CJ, Kocsis ÁT, Kiessling W. 2018. Marine invertebrate migrations trace climate change over 450 million years. *Glob. Ecol. Biogeogr.* 27:704–13

Renne PR, Sprain CJ, Richards MA, Self S, Vanderkluysen L, Pande K. 2015. State shift in Deccan volcanism at the Cretaceous-Paleogene boundary, possibly induced by impact. *Science* 350:76–78

Richter K, Haslbeck M, Buchner J. 2010. The heat shock response: life on the verge of death. *Mol. Cell* 40:253–66

Ridgwell A, Zeebe R. 2005. The role of the global carbonate cycle in the regulation and evolution of the Earth system. *Earth Planet. Sci. Lett.* 234:299–315

Ries JB. 2011. A physicochemical framework for interpreting the biological calcification response to CO_2-induced ocean acidification. *Geochim. Cosmochim. Acta* 75:4053–64

Ries JB, Cohen AL, McCorkle DC. 2009. Marine calcifiers exhibit mixed responses to CO_2-induced ocean acidification. *Geology* 37:1131–34

Romano C, Jenks JF, Jattiot R, Scheyer TM, Bylund KG, Bucher H. 2017. Marine Early Triassic Actinopterygii from Elko County (Nevada, USA): implications for the Smithian equatorial vertebrate eclipse. *J. Paleontol.* 91:1025–46

Ross PM, Parker L, Byrne M. 2016. Transgenerational responses of molluscs and echinoderms to changing ocean conditions. *ICES J. Mar. Sci.* 73:537–49

Rothman DH. 2017. Thresholds of catastrophe in the Earth system. *Sci. Adv.* 3(9):e1700906

Ruhl M, Bonis NR, Reichart G-J, Damste JSS, Kurschner WM. 2011. Atmospheric carbon injection linked to End-Triassic mass extinction. *Science* 333:430–34

Sanei H, Grasby SE, Beauchamp B. 2012. Latest Permian mercury anomalies. *Geology* 40:63–66

Scaife JD, Ruhl M, Dickson AJ, Mather TA, Jenkyns HC, et al. 2017. Sedimentary mercury enrichments as a marker for submarine large igneous province volcanism? Evidence from the mid-Cenomanian Event and Oceanic Anoxic Event 2 (Late Cretaceous). *Geochem. Geophys. Geosystems* 18:4253–75

Schaller MF, Wright JD, Kent DV. 2011. Atmospheric pCO_2 perturbations associated with the Central Atlantic Magmatic Province. *Science* 331:1404–9

Schlanger SO, Jenkyns HC. 1976. Cretaceous oceanic anoxic events: causes and consequences. *Geol. Mijnb.* 55:179–84

Schmidt A, Skeffington RA, Thordarson T, Self S, Forster PM, et al. 2016. Selective environmental stress from sulphur emitted by continental flood basalt eruptions. *Nat. Geosci.* 9:77–82

Schobben M, Joachimski MM, Korn D, Leda L, Korte C. 2014. Palaeotethys seawater temperature rise and an intensified hydrological cycle following the end-Permian mass extinction. *Gondwana Res.* 26:675–83

Schobben M, van de Velde S, Gliwa J, Leda L, Korn D, et al. 2017. Latest Permian carbonate carbon isotope variability traces heterogeneous organic carbon accumulation and authigenic carbonate formation. *Clim. Past* 13:1635–59

Schoene B, Samperton KM, Eddy MP, Keller G, Adatte T, et al. 2015. U-Pb geochronology of the Deccan Traps and relation to the end-Cretaceous mass extinction. *Science* 347:182–84

Schulte P, Alegret L, Arenillas I, Arz JA, Barton PJ, et al. 2010. The Chicxulub asteroid impact and mass extinction at the Cretaceous-Paleogene boundary. *Science* 327:1214–18

Seibel BA. 2011. Critical oxygen levels and metabolic suppression in oceanic oxygen minimum zones. *J. Exp. Biol.* 214:326–36

Self S, Schmidt A, Mather TA. 2014. Emplacement characteristics, time scales, and volcanic gas release rates of continental flood basalt eruptions on Earth. In *Volcanism, Impacts, and Mass Extinctions: Causes and Effects*, ed. G Keller, AC Kerr, pp. 319–37. Geol. Soc. Am. Spec. Pap. 505. Boulder, CO: Geol. Soc. Am.

Self S, Thordarson T, Widdowson M. 2005. Gas fluxes from flood basalt eruptions. *Elements* 1:283–87

Sibert E, Norris R, Cuevas J, Graves L. 2016. Eighty-five million years of Pacific Ocean gyre ecosystem structure: long-term stability marked by punctuated change. *Proc. R. Soc. B* 283:20160189

Silva-Tamayo JC, Lau KV, Jost AB, Payne JL, Wignall PB, et al. 2018. Global perturbation of the marine calcium cycle during the Permian-Triassic transition. *GSA Bull.* 130:1323–38

Sluijs A, van Roij L, Harrington GJ, Schouten S, Sessa JA, et al. 2014. Warming, euxinia and sea level rise during the Paleocene–Eocene Thermal Maximum on the Gulf Coastal Plain: implications for ocean oxygenation and nutrient cycling. *Clim. Past* 10:1421–39

Sokolova IM. 2013. Energy-limited tolerance to stress as a conceptual framework to integrate the effects of multiple stressors. *Integr. Comp. Biol.* 53:597–608

Sokolova IM, Lannig G. 2008. Interactive effects of metal pollution and temperature on metabolism in aquatic ectotherms: implications of global climate change. *Clim. Res.* 37:181–201

Song H, Wignall PB, Chu D, Tong J, Sun Y, et al. 2015. Anoxia/high temperature double whammy during the Permian-Triassic marine crisis and its aftermath. *Sci. Rep.* 4:4132

Spalding C, Finnegan S, Fischer WW. 2017. Energetic costs of calcification under ocean acidification. *Glob. Biogeochem. Cycles* 31:866–77

Speijer RP, Scheibner C, Stassen P, Morsi A-MM. 2012. Response of marine ecosystems to deep-time global warming: a synthesis of biotic patterns across the Paleocene-Eocene thermal maximum (PETM). *Austrian J. Earth Sci.* 105:6–16

Stapp LS, Parker LM, O'Connor WA, Bock C, Ross PM, et al. 2018. Sensitivity to ocean acidification differs between populations of the Sydney rock oyster: role of filtration and ion-regulatory capacities. *Mar. Environ. Res.* 135:103–13

Storey M, Duncan RA, Swisher CC. 2007. Paleocene-Eocene Thermal Maximum and the opening of the northeast Atlantic. *Science* 316:587–89

Stumpp M, Trübenbach K, Brennecke D, Hu MY, Melzner F. 2012. Resource allocation and extracellular acid-base status in the sea urchin *Strongylocentrotus droebachiensis* in response to CO_2 induced seawater acidification. *Aquat. Toxicol.* 110–111:194–207

Suan G, Mattioli E, Pittet B, Mailliot S, Lécuyer C. 2008. Evidence for major environmental perturbation prior to and during the Toarcian (Early Jurassic) oceanic anoxic event from the Lusitanian Basin, Portugal. *Paleoceanography* 23:PA1202

Sun H, Xiao Y, Gao Y, Zhang G, Casey JF, Shen Y. 2018. Rapid enhancement of chemical weathering recorded by extremely light seawater lithium isotopes at the Permian–Triassic boundary. *PNAS* 115:3782–87

Sun Y, Joachimski MM, Wignall PB, Yan C, Chen Y, et al. 2012. Lethally hot temperatures during the Early Triassic greenhouse. *Science* 338:366–70

Sunday JM, Bates AE, Dulvy NK. 2011. Global analysis of thermal tolerance and latitude in ectotherms. *Proc. R. Soc. B* 278:1823–30

Sunday JM, Bates AE, Dulvy NK. 2012. Thermal tolerance and the global redistribution of animals. *Nat. Clim. Change* 2:686–90

Sunday JM, Calosi P, Dupont S, Munday PL, Stillman JH, Reusch TBH. 2014. Evolution in an acidifying ocean. *Trends Ecol. Evol.* 29:117–25

Svensen H, Planke S, Malthe-Sørenssen A, Jamtveit B, Myklebust R, et al. 2004. Release of methane from a volcanic basin as a mechanism for initial Eocene global warming. *Nature* 429:542–45

Svensen H, Planke S, Polozov AG, Schmidbauer N, Corfu F, et al. 2009. Siberian gas venting and the end-Permian environmental crisis. *Earth Planet. Sci. Lett.* 277:490–500

Thibodeau AM, Ritterbush K, Yager JA, West AJ, Ibarra Y, et al. 2016. Mercury anomalies and the timing of biotic recovery following the end-Triassic mass extinction. *Nat. Commun.* 7:11147

Thomas E. 2007. Cenozoic mass extinctions in the deep sea: What perturbs the largest habitat on Earth? In *Large Ecosystem Perturbations: Causes and Consequences*, ed. S Monechi, R Coccioni, MR Rampino, pp. 1–23. Geol. Soc. Am. Spec. Pap. 424. Boulder, CO: Geol. Soc. Am.

Thomsen J, Casties I, Pansch C, Körtzinger A, Melzner F. 2013. Food availability outweighs ocean acidification effects in juvenile *Mytilus edulis*: laboratory and field experiments. *Glob. Change Biol.* 19:1017–27

Thorne PM, Ruta M, Benton MJ. 2011. Resetting the evolution of marine reptiles at the Triassic-Jurassic boundary. *PNAS* 108:8339–44

Tobin TS, Wilson GP, Eiler JM, Hartman JH. 2014. Environmental change across a terrestrial Cretaceous-Paleogene boundary section in eastern Montana, USA, constrained by carbonate clumped isotope paleothermometry. *Geology* 42:351–54

Trabucho Alexandre J, Tuenter E, Henstra GA, van der Zwan KJ, van de Wal RSW, et al. 2010. The mid-Cretaceous North Atlantic nutrient trap: black shales and OAEs. *Paleoceanography* 25:PA4201

Turgeon SC, Creaser RA. 2008. Cretaceous oceanic anoxic event 2 triggered by a massive magmatic episode. *Nature* 454:323–26

van de Schootbrugge B, Bachan A, Suan G, Richoz S, Payne JL. 2013. Microbes, mud and methane: cause and consequence of recurrent Early Jurassic anoxia following the end-Triassic mass extinction. *Palaeontology* 56:685–709

Vaquer-Sunyer R, Duarte CM. 2011. Temperature effects on oxygen thresholds for hypoxia in marine benthic organisms. *Glob. Change Biol.* 17:1788–97

Vázquez P, Clapham ME. 2017. Extinction selectivity among marine fishes during multistressor global change in the end-Permian and end-Triassic crises. *Geology* 45:395–98

Vinagre C, Leal I, Mendonça V, Madeira D, Narciso L, et al. 2016. Vulnerability to climate warming and acclimation capacity of tropical and temperate coastal organisms. *Ecol. Indicat.* 62:317–27

Vörös A, Kocsis ÁT, Pálfy J. 2016. Demise of the last two spire-bearing brachiopod orders (Spiriferinida and Athyridida) at the Toarcian (Early Jurassic) extinction event. *Palaeogeogr. Palaeoclimatol. Palaeoecol.* 457:233–41

Whiteley NM. 2011. Physiological and ecological responses of crustaceans to ocean acidification. *Mar. Ecol. Prog. Ser.* 430:257–71

Wignall PB, Hallam A. 1992. Anoxia as a cause of the Permian/Triassic mass extinction: facies evidence from northern Italy and the western United States. *Palaeogeogr. Palaeoclimatol. Palaeoecol.* 93:21–46

Xu W, Ruhl M, Hesselbo SP, Riding JB, Jenkyns HC. 2017. Orbital pacing of the Early Jurassic carbon cycle, black-shale formation and seabed methane seepage. *Sedimentology* 64:127–49

Zachos JC, Röhl U, Schellenberg SA, Sluijs A, Hodell DA, et al. 2005. Rapid acidification of the ocean during the Paleocene-Eocene thermal maximum. *Science* 308:1611–15

Zachos JC, Wara MW, Bohaty S, Delaney ML, Petrizzo MR, et al. 2003. A transient rise in tropical sea surface temperature during the Paleocene-Eocene Thermal Maximum. *Science* 302:1551–54